POLITEHNICA UNIVERSITY TIMIŞOARA
Civil Engineering Faculty
Department of Steel Structures and Structural Mechanics

ADAPTIVE REUSE OF AN OLD STEEL HALL

Author: **Horia-Dan FECHETE, Civ. Eng.**

Supervisor: **Professor Dan DUBINĂ, Ph.D.**

Universitatea Politehnica Timişoara, Romania

Study Program: **SUSCOS_M**

Academic year: **2017/2018**

ADAPTIVE REUSE OF AN OLD STEEL HALL

By

Horia-Dan FECHETE

Thesis submitted in partial fulfillment of the requirements for the degree of

MASTER OF SCIENCE

in

CIVIL ENGINEERING

European Erasmus Mundus Masters Course

Sustainable Construction Under Natural Hazards and Catastrophic Events

February 2018

Keywords: Adaptive reuse, extension of the service life, structural upgrade, rehabilitation, non-destructive tests, advanced analysis

MEMBERS OF THE JURY

President: **Professor Dan DUBINĂ, Ph.D.**
Member of the Romanian Academy
(Thesis Supervisor)
Politehnica University Timişoara
Str. Ioan Curea, 1
300224, Timişoara, Timiş, Romania

Members: **Professor Adrian CIUTINA, Ph.D.**
Politehnica University Timişoara
Str. Ioan Curea, 1
300224, Timişoara, Timiş, Romania

Professor Florea DINU, Ph.D.
Politehnica University Timişoara
Str. Ioan Curea, 1
300224, Timişoara, Timiş, Romania

Professor Viorel UNGUREANU, Ph.D.
Politehnica University Timişoara
Str. Ioan Curea, 1
300224, Timişoara, Timiş, Romania

Assoc. Professor Adrian DOGARIU, Ph.D.
Politehnica University Timişoara
Str. Ioan Curea, 1
300224, Timişoara, Timiş, Romania

Secretary: **Asst. Professor Ioan MĂRGINEAN, Ph.D.**
Politehnica University Timişoara
Str. Ioan Curea, 1
300224, Timişoara, Timiş, Romania

ACKNOWLEDGMENTS

This thesis was developed during my activity in SUSCOS (2016-2018) at the Department of Steel Structures and Structural Mechanics (CMMC) and the Centre of Excellence in the Mechanics of Materials and Safety of Structures (CEMSIG) from Universitatea Politehnica Timisoara in Romania.

I would like to express my deepest gratitude towards my supervisor, Professor Dan Dubină, PhD, Member of the Romanian Academy, for his continuous and invaluable guidance provided throughout my research activity and for offering me the opportunity of working on the PROGRESS research program.

I would like to thank the entire academic staff of the CMMC Department for their support and for being such good colleagues. Especially, I would like to thank Professor Adrian Ciutina for organizing our stay in Timisoara, Assoc. Professor Adrian Dogariu for his precious advice on the numerical analysis, Eng. Ovidiu Abrudan for his help with the laboratory work and, last but not least, my office colleagues, Dominiq Jakab, Adina Vătăman and Simina Sabău, for their help and friendship.

Moreover, I am grateful to the professors that are coordinating this SUSCOS Master Program, Professor František Wald, Professor Dan Dubină, Professor Raffaele Landolfo, Professor Luís Simões da Silva and Professor Jean-Pierre Jaspart, as well as to all the other professors involved in this program.

Finally, I would like to thank my family and friends for their continuous support and help. Without them, none of this would have been possible.

ABSTRACT

Nowadays, great importance is given to limiting the use of non-renewable resources and decreasing the impact on the environment. The reuse of steel structures is becoming more efficient than recycling steel, which implies additional environmental burden and higher production costs. Steel structures can be reused in different ways, either by incorporating into a new structure the steel elements obtained through dismantling old buildings or by rehabilitating an old steel structure to make it meet the current design requirements.

The aim of the thesis is the adaptive reuse of the CMMC Department steel hall (60 years old) by extending its service life through a structural upgrade. The main issue is due to the change of codes and norms from the time of initial design; the current design codes operate with increased climate and seismic loads. Moreover, a part of the primary structure was severely damaged during a recent storm, making the rehabilitation even more important and urgent. The structure was inspected in order to observe the imperfections and existing damage; the welds were evaluated by dye penetrant inspection in order to assess if they had been damaged over time. Non-destructive hardness tests were performed on the structural elements in order to determine the steel grade of the material. The proposed technical solution has been validated through an advanced analysis.

TABLE OF CONTENTS

LIST OF FIGURES

LIST OF TABLES

1 INTRODUCTION

1.1 Overview

Nowadays, when dealing with old steel structures, the current practice is to demolish and recycle them. However, the process of recycling implies high costs and has a great impact on the environment. As the reuse of steel structures is more efficient than recycling in terms of costs and environmental burden, it is becoming more and more popular [1]. Steel structures can be reused entirely or partially (only some elements are reused from the structure). Depending on the location, the reuse can be made in-situ or by dismantling and relocation to a new site [2]. The material flow is presented in case of recycling (See Figure 1.1), partial reuse (See Figure 1.2) and full reuse (See Figure 1.3).

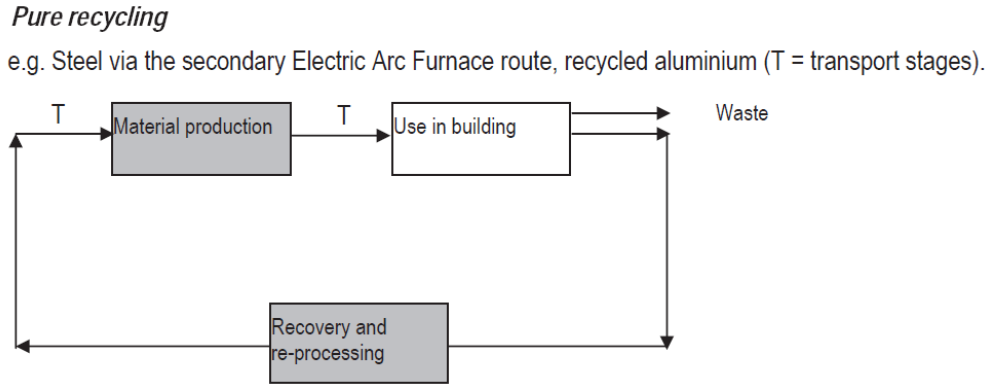

Figure 1.1 Material flow in case of recycling [2]

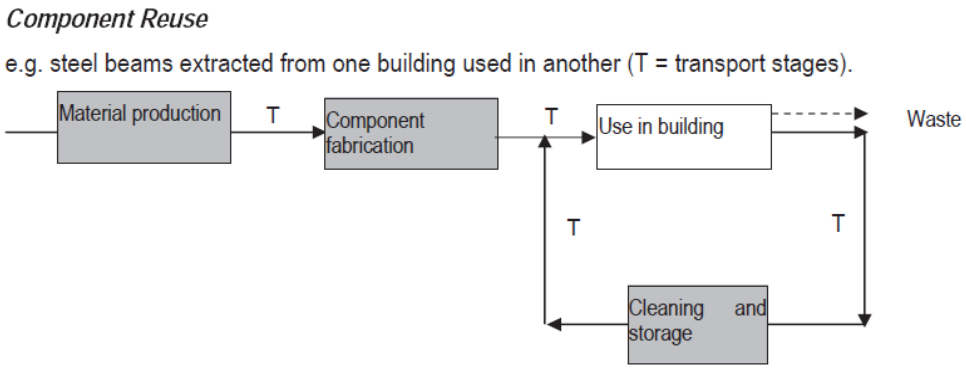

Figure 1.2 Material flow in case of partial reuse [2]

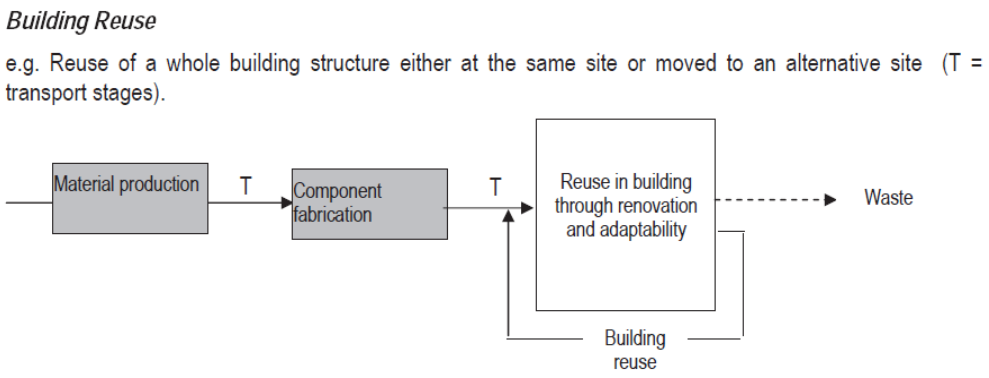

Figure 1.3 Material flow in case of full reuse [2]

1.2 Research framework (RFCS-02-2016, Proposal No. 747847, "PROGRESS")

The aim of the "Provisions for Greater Reuse of Steel Structures" (PROGRESS) project is to provide methodologies, tools and recommendations regarding the reuse of steel components from new and existing buildings. The main focus of the project is the design, with the future purpose of dismantle and reuse, of roof cladings, transversal frames, trusses and secondary elements of single-storey frame buildings [3].

The particular objectives of the project are to:

- Extend the service life of building elements by reusing them after their removal from the original structure;
- Reduce the raw material and energy consumption of steel sector, and embodied impacts of the steel buildings;
- Develop the design guidance for the successful planning of assembled structures with reused elements and the buildings that will be deconstructed in the future to maximize the reuse potential of their elements and systems;
- Establish the quality verification process, testing and evaluation methods, and develop the related services and business models in order to enable reuse of building elements recovered from the demolition or renovation activities;
- Improve the overall building performance by improvement of multi-material and multifunctional hybrid systems reusability;
- Demonstrate the reuse process/technologies, related circular economy models and environmental benefits on selected case studies;
- Involve all actors in the product supply chain to actively participate and contribute to the attainment of the project objectives by direct collaboration and workshops [3].

The project aims to support the transformation to a more resource-efficient economy in Europe. The target of European Waste Directive is that 70% of construction and demolition waste (CDW) should be recycled, reused and/or recovered by 2020. The focus area to achieve this goal is highlighted in the waste hierarchy (See Figure 1.4) [3].

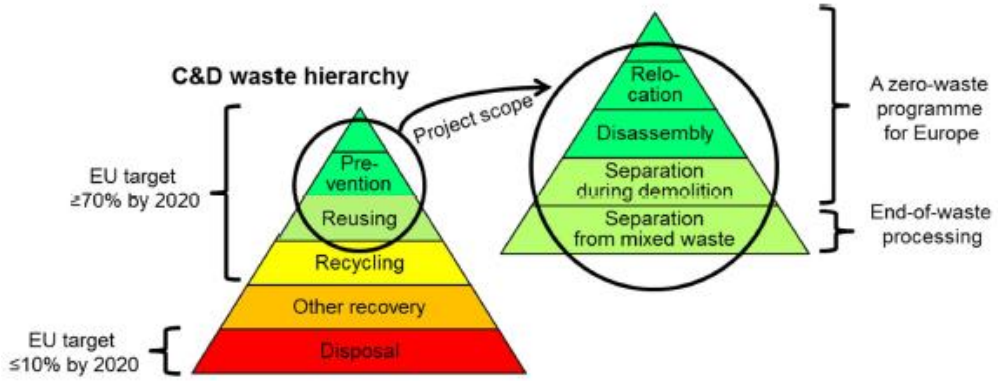

Figure 1.4 Project scope in the terms of waste prevention and material recovery [3]

To facilitate the reuse process, it is necessary to identify the major actors in the supply chain and the way they interact (See Figure 1.5) in order to have a clear understanding of the role of each actor and how the reuse can be achieved at different levels of the supply chain. Recommendations will be provided for each of the actors concerning design, deconstruction, maintenance, storage, handling, remanufacturing and other activities associated with the exploitation of the economic potential of reuse products [3].

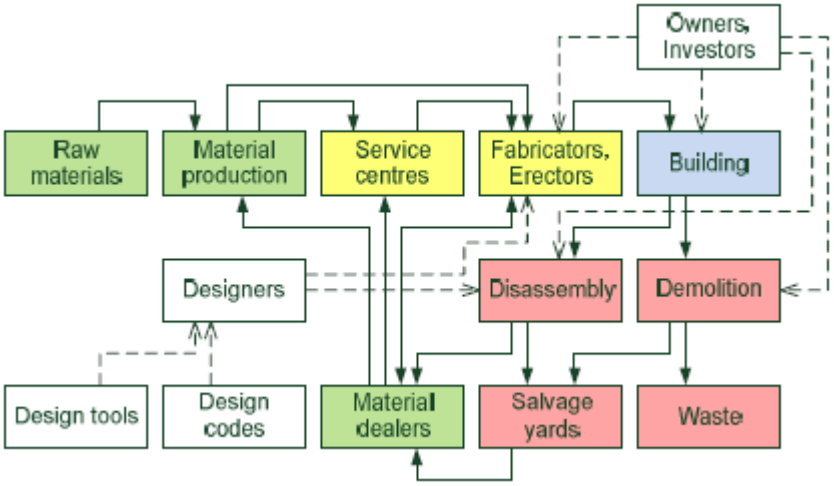

Figure 1.5 Major actors in the reuse process and their interaction [3]

The PROGRESS project is carried out with the partners below:

- TEKNOLOGIAN TUTKIMUSKESKUS VTT OY (FI)
- THE STEEL CONSTRUCTION INSTITUTE LBG (UK)
- RUUKKI CONSTRUCTION OY (FI)
- RHEINISCH-WESTFAELISCHE TECHNISCHE HOCHSCHULE AACHEN (DE)
- UNIVERSITATEA POLITEHNICA TIMISOARA (RO)
- CONVENTION EUROPEENNE DE LA CONSTRUCTION

The research activity of the research project consists of nine work packages, as follows:

Work Package 1: Reuse potential of steel-intensive single-storey buildings

This WP reviews the experiences from the successful reuse and deconstruction projects collected by the project partners and from the practitioners in the building industry (through the interviews or workshops). The results will be summarized in the form of factsheets (Task 1.1, Deliverable 1.1) and further analyzed to support the development of the assessment of the reuse potential of single-storey steel-intensive buildings and their components (Task 1.2 and 1.3, Deliverable 1.2). The summary of regulatory barriers and opportunities will be produced in Task 1.4 (Deliverable 1.3).

Work Package 2: Reuse of steel and steel-based components from existing buildings

This WP addresses the issues connected to the reuse of elements from the deconstructed buildings. The safe and efficient deconstruction process supported by pre-demolition audits will be developed in Task 2.1and 2.2 (Deliverable 2.1). Tasks 2.3 and 2.4 will propose the methods for the assessment of suitability of materials and elements for the reuse including the recommendations for their modification/adaptation to fit in the new design (Deliverable 2.2). The material and elements quality verification/testing protocol will be developed in Task 2.5 (Deliverable 2.3).

Work Package 3: Design for the future reuse

Technical recommendations for the increase of reusability of the components will be provided on component design level (Task 3.1, Deliverable 3.1) and building design level (Task 3.2, Deliverable 3.2). Moreover, the gaps in the current Building Information Modelling (BIM) definitions and software support will be addressed to enable the smooth transfer of all of the relevant information from one building to another (Task 3.3, Deliverable 3.3).

Work Package 4: Novel hybrid systems for envelopes of single-storey steel-framed buildings

The WP aims at novel hybrid solutions for envelopes of single-storey buildings, either new buildings or renovation projects that improves the thermal performance of an entire building, service life of envelopes and reusability of solutions themselves. WP4 will benchmark the product development process from the conceptualization phase to a pilot product phase of a hybrid envelope solution of single-storey buildings that improves reusability. New hybrid solution and joining methods will be proposed in Task 4.1 (Deliverable 4.1).The performance of the hybrid solution will be confirmed by testing of the elements (Task 4.2, Deliverable4.2) and its connections (Task 4.3, Deliverable 4.3) and the product will be pilot tested on the on CUBE DemoHouse at RWRH (Task 4.4, Deliverable 4.4).

Work Package 5: Environmental and economic benefits of reuse in the single-storey buildings

Approaches to study environmental and economic benefits of reuse of single-storey buildings will be developed / improved and the benefits quantified. A methodology to quantify and declare environmental benefits of reused elements will be developed (Task 5.1, Deliverable 5.1), resulting in recommendations on the circularity and LCA methodologies to employ within the case-studies in subsequent WP7. In parallel, Task5.2 & Deliverable 5.2 will be dedicated to estimating the economic potential of steel-based elements reuse in SSBs. Cost minimization / residual-value maximization will be achieved by effective use of quality verification and exploitation of the design procedures (including ICT and BIM).

Work Package 6: Design recommendations

The guidance developed in this WP will include recommendations for primary and secondary structural steel products and for hybrid, steel-based envelope products and systems of existing buildings (Task 6.1, Deliverable 6.1) and future buildings (Task 6.2, Deliverable 6.2). It will provide recommendations for all actors in the supply chain, i.e. demolition contractors, steelwork contractors, steel stockholders and building designers. The design guidance will be published as part of a new series of European Design Manuals that will be launched by ECCS in 2016-2020.

Work Package 7: Case studies

This WP will provide benchmark of demolition, classification and testing/verification protocols developed in WP 2 on a real deconstructed building (Task 7.1, Deliverable 7.1) including the laboratory tests to identify mechanical and chemical properties of the materials. The design case studies in Task 7.2 and 7.3 will cover the most common reuse situations (a) when the new building is designed from elements originating from a different building(s) in the same location, (b) when the building is relocated over a greater distance and redesigned to match different conditions (Deliverable 7.2), (c) when the building is designed to maximize its deconstruction efficiency and reuse potential in the future (Deliverable 7.3).

Work Package 8: Communication and dissemination

The project outcomes (especially from WP 6 and WP 7) will be disseminated through the workshops, internet presentations, newsletters and publications. The workshops and interviews will also provide a valuable feedback for the proposed assessment methods and protocols in WP 2 to 5.

Work Package 9: Coordination

Comprehensive overview (Deliverable D9.1), periodical reports, financial statements, progress meetings and other project coordination tasks are included in Task 9.1. The management of WPs belongs to Task 9.2 [3].

The interaction of the Work Packages and Tasks is shown graphically in Figure 1.6. The two major areas of the application of PROGRESS project outcomes are the increased reuse of elements recovered from the deconstruction of existing buildings and the improvement of the design of new buildings and elements so that they are more easy to deconstruct and it is easier to recover and reuse their constituent parts The relevant Tasks are indicated by dotted line in Figure 1.6 [3].

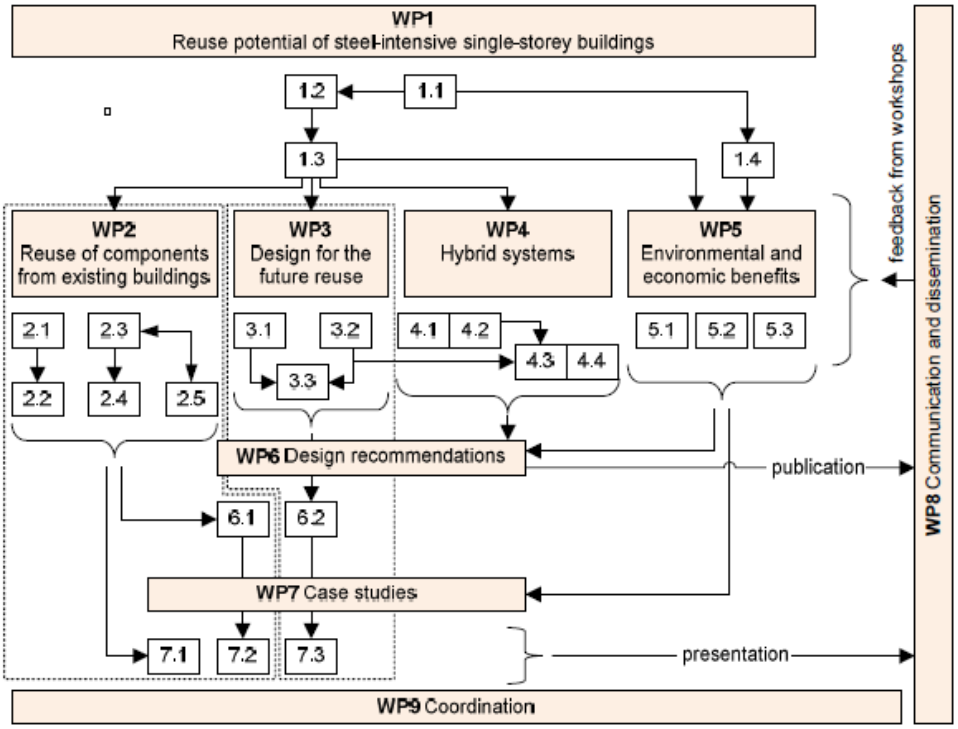

Figure 1.6 Work Packages, Tasks and their interactions [3]

The topic treated in this thesis falls within the framework of Work Package 7.

The major reuse cases considered in the PROGRESS project are described in Figure 1.7.

	Same layout	**Different layout** Modification/adaptation can be needed due to different individual member loading	
	Relocated reuse Modification/adaptation can be needed due to different external conditions and regulatory requirements.		**In-situ reuse**
Frames	(A) Deconstruction and re-assembly on a new site.	(B) Several (or all) frames are integrated into the new building layout	
		(C) Reuse of individual elements cut from the frame (e.g. sections) on different site(s)	(D) Reuse of individual elements cut from the frame (e.g. sections) in the new building on the same site
Secondary structure		(E) Reuse of individual elements on different site(s)	(F) Deconstruction and reuse of elements in a different configuration
Envelope			

Figure 1.7 Basic reuse cases in the scope of the PROGRESS project [3]

The case studies within the framework of this project are presented in Table 1.1.

Table 1.1 Case studies within the framework of the PROGRESS research project [4]

Case Study	Image	Brief description
1		**NTS building, Thirsk, UK** The original order for the building was cancelled in 2008 and the elements were stored. The new building was erected in 2017 by reusing a quarter of the steelwork of the original building.
2		**Deconstruction and relocation of a warehouse and office building in Slough, UK** The structure was built in 2000 and relocated in a different layout in 2015.
3		**Single storey industrial hall converted into multi-storey office building in Timisoara, Romania** The building was erected in the 1960s as a single storey industrial hall of steel structural elements with crane and converted into a five-storey office building in 2004.
4		**Conversion of the former heat and power plant of RWTH Aachen University into a seminar building** Following the closure of the RWTH heat and power plant in the 1990s, the decision was made to transform it into a seminar building by adapting the structure to meet the new functional requirements.

5		**Design of the in-situ rehabilitation of the Steel Structures Laboratory of PUT in Timisoara, Romania** The structure was erected in 1959, consisting of truss elements. Part of the structure was severely damaged in 2017 by a storm.
6		**The design of a relocated steel industrial hall in Timisoara, Romania** The structure was designed in 2008 as a ***standard kit*** to be adapted for different locations and applications. It was erected in 2009 and relocated for reuse in 2017.
7		**Deconstruction and relocation of a warehouse and office building in Copăceni, Romania** The building was erected in 2004 in Craiova, consisting of a two-storey office area and a warehouse. In 2012, it was moved to Copăceni (227 km east of Craiova) and one more bay was added to the warehouse.
8		**Bus station Schiphol – Nord, Netherlands** The original building was erected in 1958 and was used as a hangar by the Rotterdam Airport until the late nineties. In 2003, the structure was reused as a hangar for seven years by the Rotterdam Detention Center. In 2015, it was reused again as a bus station in Schiphol.

9		**Deconstruction and relocation of a steel canopy in Otočcu, Croatia** The original structure was erected in Pula and was relocated for reuse in 2011 in Otočcu, 266 km away.

Among these case studies, Case Study no. 5 is treated in this thesis. As the structure of the hall was designed and erected in 1959, it does not meet the requirements of the current design codes. By rehabilitating the structure, its service life is extended, therefore reusing the structure, rather than demolishing it in order to build a new one. The reuse is made in-situ by keeping the same layout. With the exception of the damaged girders, the entire main and secondary structure is reused, with the addition of new elements.

1.3 Scope

Within the framework of the PROGRESS research program, the objective of the thesis is the adaptive reuse of the CMMC Department steel hall by extending its service life through a structural upgrade. The main issue is due to the change of codes and norms from the time of initial design; the current design codes operate with increased climate and seismic loads. Moreover, a part of the primary structure was severely damaged during a recent storm, making the rehabilitation even more important and urgent.

Adaptive reuse of buildings can be defined as "*the process of adapting and modifying older buildings, some of which may in fact be considered obsolete, to perform new desired uses or functions. In some cases, the occupancy usage may be fundamentally and sometimes radically changed. The process, which can actually be quite complex, allows buildings, in some instances, to be re-configured, enabling structures to perform new and sometimes quite different functions and/or face different action effects, climate change included.*"

Within the framework of this thesis, the adaptive reuse refers to structurally upgrading the hall without interrupting the laboratory activities during the application of the rehabilitation solution. Due to this, the aim is not to provide the most economical solution (which would be the demolition of the old hall and the erection of a new one made from hot-rolled profiles, but for which the laboratory work cannot be performed), but to provide a rehabilitation solution (with reasonable costs) for which the functioning of the laboratory hall does not need to be stopped.

1.4 Methodology

The objective of the thesis is accomplished through the following steps:

1. Performing in-situ measurements and non-destructive tests for the material and the welds in order to determine the steel grade of the structural elements and to assess if the welds have been damaged over time;

2. Evaluation of the level of structural safety of the initial structure according to the current design codes;
3. Proposal of a rehabilitation solution;
4. Validation of the proposed rehabilitation solution through a numerical analysis.

2 DESCRIPTION OF THE BUILDING

2.1 General overview of the structure

The building is located in Timisoara and it belongs to the Department of Steel Structures and Structural Mechanics from the Faculty of Civil Engineering of Timisoara. It is used as testing laboratory [5].

The building was erected in 1959. The main structural system is composed of truss girders and columns. The walls are made from masonry combined with continuous glazed surfaces. In the longitudinal direction, X braces are provided in the last bay. The roof is made of timber boards (inner face), having lightweight thermal insulation and standing seam roof, being supported on truss purlins at a distance of 2.5 m. No bracing system exists in the roof level [5].

The original drawings and design are not available, so all the dimensions were determined by in-situ measurements. The structure has 5 bays of 6 m (a total of 30 m length), the span of the transversal frame is of 10.5 m and the height of the structure is 7 m at the eaves and 7.55 m at the ridge, with a roof slope of 10%. The stages of erection of the hall are presented in Figure 2.1 and Figure 2.2 [5].

Figure 2.1 Erection of the steel structure [5]

Figure 2.2 The Department of Steel Structures and Structural Mechanics (right) and the laboratory building (left) done in 1959 [5]

Figure 2.3 presents schematically the 3D view of the structure.

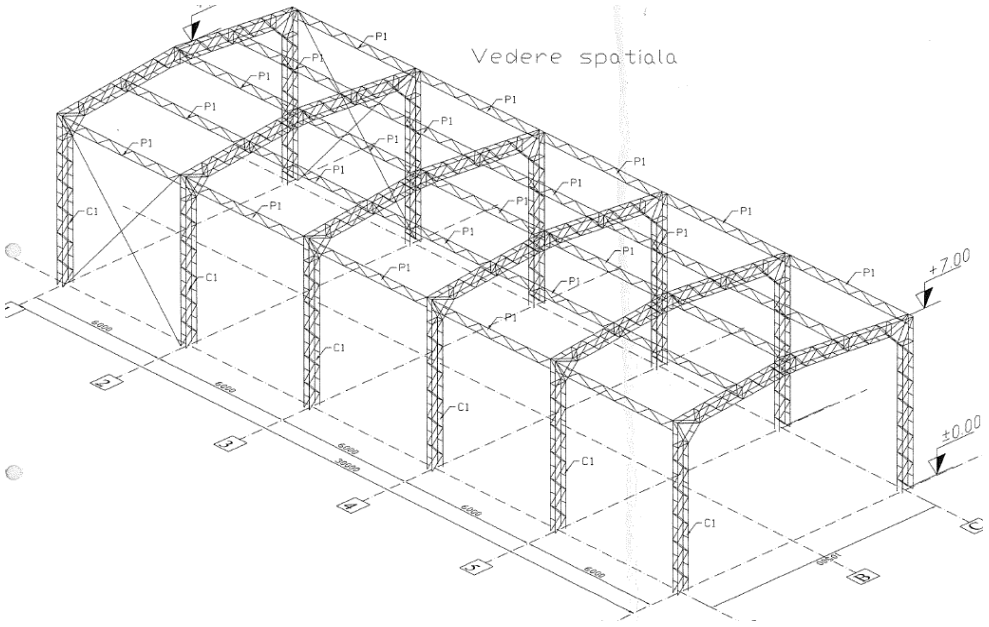

Figure 2.3 The 3D view of the structure and global dimensions [5]

The girders and columns of the transversal frames have an identical cross-section, as shown in Figure 2.4. The dimensions of the built-up cross-sections are of 250 x 500 mm, combining laced and battened for the built-up members. The built-up cross-section is composed of 4 L45x45x5 angle profiles placed at the corners of the cross-section connected on the lateral faces (the dimensions of 500 mm) by diagonals, round steel bars of 16 mm diameter, welded to the angle profiles. On the other two faces of the cross-section (the dimensions of 250 mm),

the angle profiles are connected with steel plates, with the cross-section of 60x8 mm, placed at each 500mm [5].

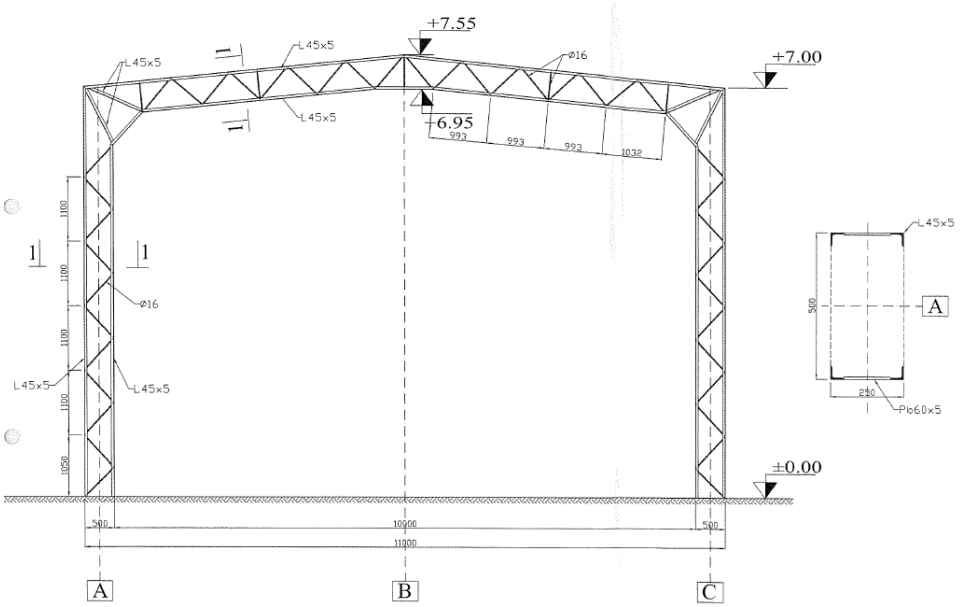

Figure 2.4 The transversal frame and the cross-section of the girders and columns [5]

In the case of purlins (See Figure 2.5), the top chords are made from cold-formed steel plain channel profile with the cross-section of U100x40x4, the bottom chords are made of angle profiles with the cross-section of L45x45x5, rotated at 45°, and the diagonal bars are made from round steel bars having the cross-section of 16mm, welded to the chords [5].

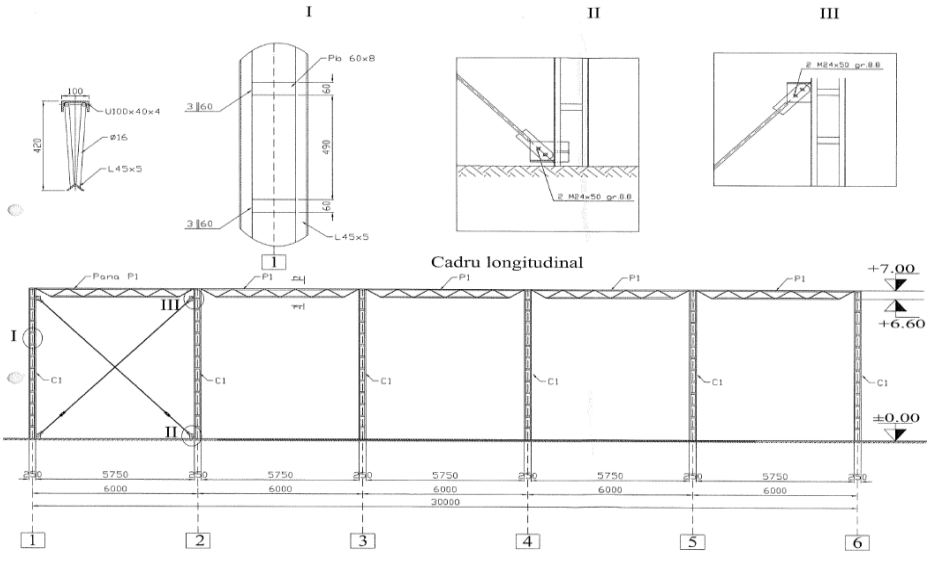

Figure 2.5 The longitudinal frame, the cross-section of the purlin and specific details [5]

Due to the fact that the original documents are not available, the steel grade was determined by performing non-destructive hardness tests on the structural elements. Following the tests, it was concluded that the steel grade of the structural elements is S235. The tests are presented in Paragraph 3.1.

The welds were evaluated by dye penetrant inspection in order to assess if they had been damaged over time. After performing the tests, it resulted that the welds did not present any damage. The tests are presented in Paragraph 3.2.

2.2 Background of the codes available at the time of the design

At the time, the design of structures was performed according to the allowable stress design (ASD) method, as opposed to the limit state design (LSD) method, which is currently used. The difference between the two methods is reflected in the different values of the partial safety factors used for the loads and material. The comparison between the two methods is highlighted in Table 2.1 and Table 2.2.

Table 2.1 Partial safety factors for loads in the case of the ASD and LSD methods [6]

Design situation / Load case	Fundamental		Seismic	
	ASD	LSD	ASD	LSD
Dead load (G)	1	1.35	1	1
Snow load (S)	1	1.5/1.05	1	0.4
Wind load (W)	1	1.05/1.5	0	0
Seismic load (A)	0	0	1	1

Table 2.2 Partial safety factors and allowable/design strengths for the material in the case of the ASD and LSD methods [7]

Design method / Design situation	Partial safety factors		Allowable/design strengths for OL37/S235 [N/mm^2]		Allowable/design strengths for OL52/S355 [N/mm^2]	
	ASD	LSD	ASD	LSD	ASD	LSD
Fundamental	1.6	1	150	235	225	355
Seismic	1.23	1.1	195	214	293	323

2.3 Damage suffered by the structure after the September 2017 storm

The frames damaged by the storm are the frames in axis 4 (significant plastic deformation of the girder) and the frame in axis 5 (the girder is only slightly deformed). The state of the structure following the storm is presented below.

The top view of the hall is presented in Figure 2.6. It can be observed how the roof from the adjacent higher building was carried by the storm on the roof of the hall. This is the cause of the damage of the structure; the roof of the hall was smashed by the roof of the higher building, being subjected to a load greater than the bearing capacity of the structure.

Figure 2.6 Top view of the hall after the storm

The general view of the frame in axis 4 is presented in Figure 2.7. It can be observed how the girder experienced severe plastic deformations in the regions close to the nodes, as well as the damage suffered by the roof.

Figure 2.7 The girder from the frame in axis 4 after the storm

The damage in the right-hand side of the girder from the frame in axis 4 is presented in the following. The excessive deformation of the girder angles and the buckling of the diagonals can be noticed in Figure 2.8. The cracking of the continuity weld of the angles is presented in Figure 2.9. The buckling of the diagonals can also be noticed in Figure 2.10.

Figure 2.8 Deformation of the girder angles and buckling of diagonals

Figure 2.9 Cracking of the continuity weld of the angles

Figure 2.10 Buckling of diagonals

The same damage (cracking of weld and buckling of diagonals) occurred in the left-hand side of the girder from the frame in axis 4, as well as in the girder from the frame in axis 5 (both right and left-hand side).

3 ASSESSMENT OF THE INITIAL STRUCTURE

The assessment of the initial structure was performed by following the steps presented in Figure 3.1.

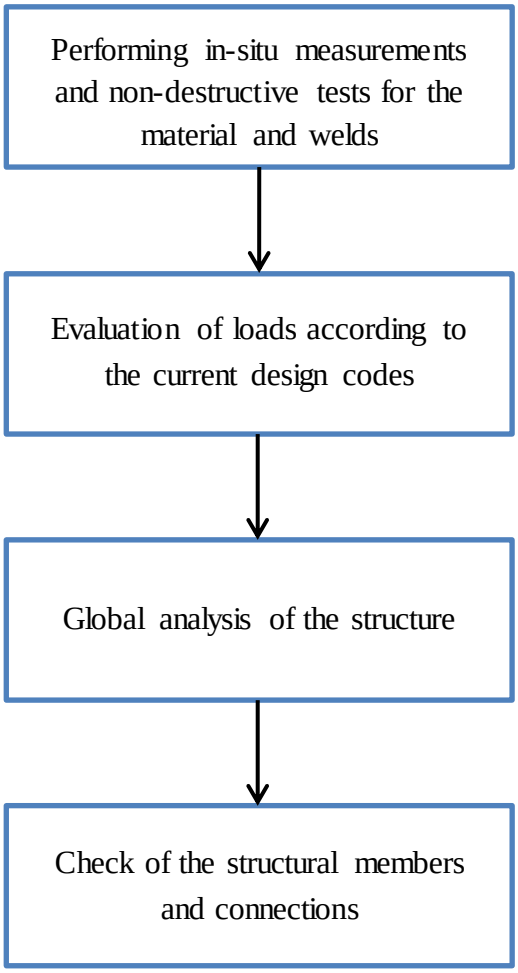

Figure 3.1 Flow chart for the assessment of the initial structure

3.1 Hardness tests for the material

In order to determine the steel grade of the material, non-destructive hardness tests were performed on the structural elements. The equipment used for the tests is presented in Figure 3.2.

Figure 3.2 Equipment used for the non-destructive hardness tests

One of the surfaces on which the tests were performed is presented in Figure 3.3. In order to perform the test, the paint must be removed from the surface of the element. Subsequently, the surface must be polished in order to obtain a surface as smooth as possible.

Figure 3.3 Surface for the non-destructive hardness tests

The procedure of performing the test is presented in Figure 3.4. The "pen" of the equipment is placed perpendicularly on the prepared surface. Afterwards, pressure is applied on the "pen" in order to generate an impulse. Finally, the result (the ultimate tensile strength) is displayed.

Figure 3.4 Procedure of performing the hardness test

For a surface, the procedure must be performed 5 times, and the result is given as the mean of the 5 values. The results of one test are presented in Figure 3.5.

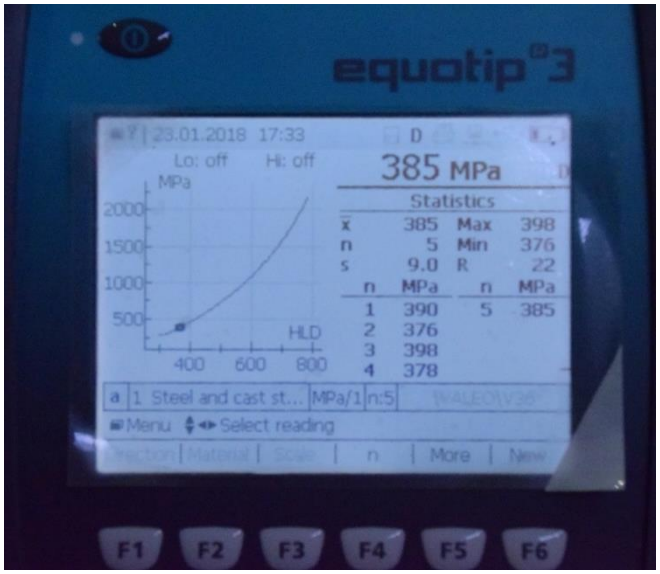

Figure 3.5 Results of the hardness test

Similar results were obtained for the other tests. As the value of the ultimate tensile strength is 385MPa, it was concluded that the steel grade of the material is S235.

3.2 Dye penetrant inspection of the welds

In order to determine if the welds had been damaged over time, they were evaluated by dye penetrant inspection. The equipment used for the tests consists of a cleaner, a penetrant and a developer.

The locations of the inspected welds are presented in Figure 3.6. The welds were inspected on both sides of the frames in axes 4, 5 and 6.

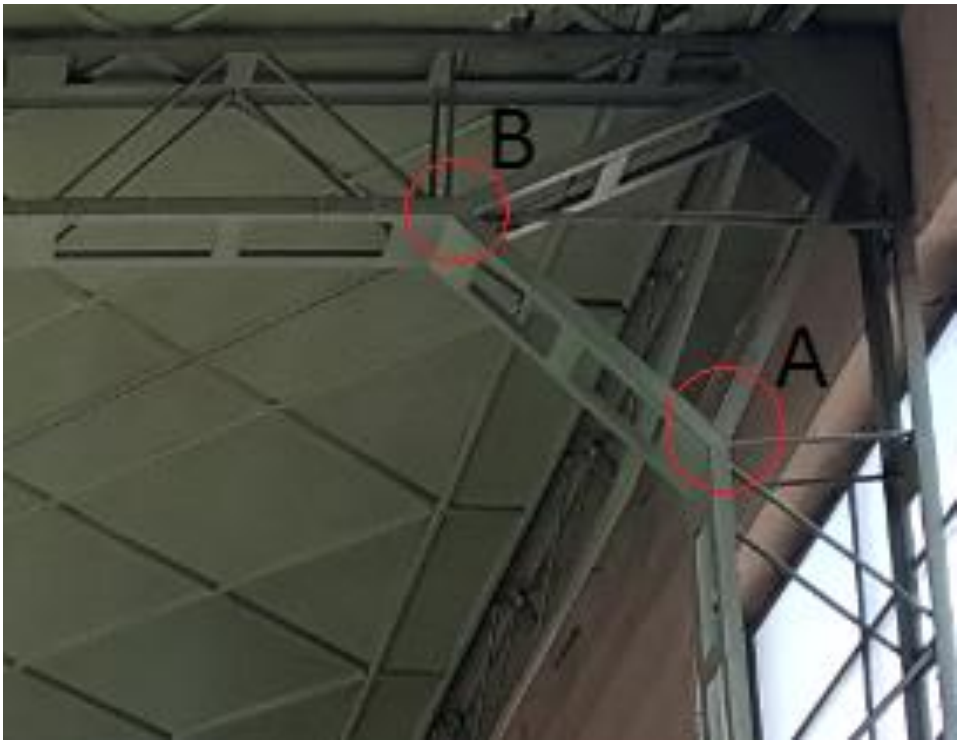

Figure 3.6 Locations of the inspected welds

Two of the surfaces on which the tests were performed are presented in Figure 3.7. In order to perform the test, the paint must be removed from the surface of the element (weld). Subsequently, the surface must be cleaned by applying the cleaner.

(a) Zone A *(b) Zone B*

Figure 3.7 Surfaces for the dye penetrant inspection

After the surface has been properly cleaned, the penetrant is applied, as presented in Figure 3.8. The penetrant must remain on the surface long enough for it to soak into any potential flaws.

Figure 3.8 Application of the penetrant

Afterwards, the excess penetrant is removed from the surface and the developer is applied (See Figure 3.9).

(a) Zone A *(b) Zone B*

Figure 3.9 Application of the developer

Finally, the surface is inspected. Due to the fact that no trace of the penetrant is visible on the surface, it results that the welds do not present any damage. The same results were obtained in case of all the welds that were tested.

3.3 Evaluation of loads according to the current design codes

3.3.1 Dead load

The dead load is given by the self-weight of the roof: $g_k = 0.3\text{kN}/m^2$.

3.3.2 Live load

A maintenance live load was considered, according to SR EN 1991-1-1/NA: $q_k = 0.5\text{kN}/m^2$.

3.3.3 Snow load

The snow load was computed according to CR-1-1-3-2012, considering 2 cases: 1 case of undrifted snow and 1 case of drifted snow. The drifting of the snow occurs in the region close to the new hall, as well as in the region close to the faculty building.

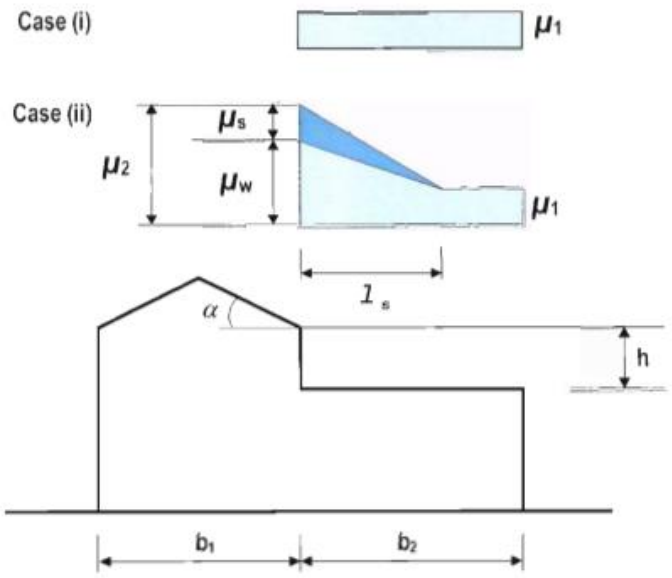

Figure 3.10 Snow load shape coefficients for roofs abutting to taller construction works [8]

In the case of the undrifted snow, the value of the load is computed below:

$g_{Is} = 1$ (importance − exposure Class III)

$\mu_1 = 0.8$ ($\alpha = 5.71° < 30°$, where α is angle of the roof)

$C_e = 1$ (normal exposure)

$C_t = 1$

$s = 1.5\text{kN}/m^2$ (for Timisoara)

$s_k = g_{Is} \cdot \mu_1 \cdot C_e \cdot C_t \cdot s = 1.2kN/m^2$

In the case of the drifted snow, for the region close to the faculty building, (frames in the axes 4,5 and 6), the value of the load is computed below:

$h = 5m$

$b_1 = 10m$

$b_2 = 30.25\text{m}$

$l_s = 2\text{h} = 10\text{m}\ (5\text{m} < l_s < 15\text{m}, b_2 > l_s)$ – the drift length

$\mu_1 = 0.8$

$\mu_s = 0\ (\alpha < 15°, \text{where } \alpha \text{ is the angle of the higher building roof})$

$g = 2\text{kN}/m^3$

$\mu_w = (b_1 + b_2)/2\text{h} = 4.025 < 6.67 = \text{g} \cdot \text{h/s}, \text{but } 0.8 \leq \mu_w \leq 4 \Rightarrow \mu_w = 4$

$\mu_2 = \mu_s + \mu_w = 4$

$s_{k,2} = g_{Is} \cdot \mu_2 \cdot C_e \cdot C_t \cdot s = 6kN/m^2$ – load value at the beginning of the drift length

$s_{k,1} = g_{Is} \cdot \mu_1 \cdot C_e \cdot C_t \cdot s = 1.2kN/m^2$ – load value at the end of the drift length

In the case of the drifted snow, for the region close to the new hall, (frames in the axes 1 and 2), the value of the load is presented below:

$s_{k,2} = 4.2kN/m^2$ – load value at the beginning of the drift length

$s_{k,1} = 1.2kN/m^2$ – load value at the end of the drift length

$l_s = 5\text{m}$ – the drift length

3.3.4 Wind load

The wind load was computed according to CR-1-1-4-2012, considering 2 cases: 1 case of longitudinal wind (direction of the wind parallel to the ridge) and 1 case of transversal wind (direction of the wind perpendicular to the ridge). The wind load was computed considering the two halls (old one and new one) as a single building.

The terrain is category IV (urban regions).

$z_0 = 1\text{m}$

$z_{min} = 10\text{m}$

$\sqrt{b} = 2.12$

$k_r^2(z_0) = 0.054$

$h = 9.65\text{m} < z_{min} \Rightarrow \text{z} = z_{min} = 10\text{m}$

$$I_v(z) = \frac{\sqrt{b}}{2.5 \cdot ln\left(\frac{z}{z_0}\right)} = 0.368$$

$c_{pq}(z) = 1 + 7 \cdot I_v(z) = 3.576$

$$c_r^2(z) = k_r^2(z_0) \cdot \left[ln\left(\frac{z}{z_0}\right)\right]^2 = 0.286$$

$q_b = 0.6\text{kN}/m^2$ (for Timisoara)

$q_p(z) = c_{pq}(z) \cdot c_r^2(z) \cdot q_b = 0.61 kN/m^2$

$g_{Iw} = 1$ (importance − exposure Class III)

$w_e = g_{Iw} \cdot c_{pe} \cdot q_p(z)$

In the case of the longitudinal wind, the value of the wind load on the roof is computed below:

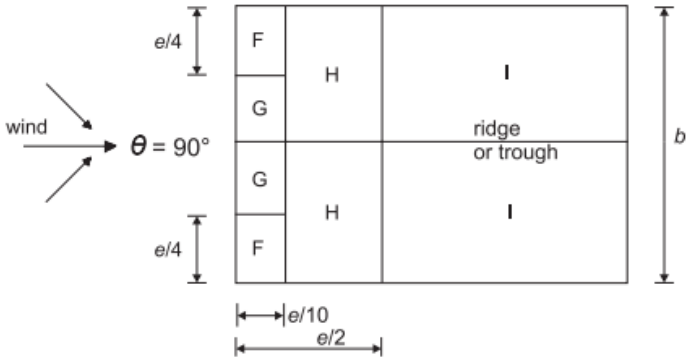

Figure 3.11 Distribution of wind pressure/suction zones on the roof in case of longitudinal wind [9]

$c_{\mathrm{pe},10,\mathrm{F}} = -1.6$

$c_{\mathrm{pe},10,\mathrm{G}} = -1.3$

$c_{\mathrm{pe},10,\mathrm{H}} = -0.7$

$c_{\mathrm{pe},10,\mathrm{I}} = -0.593$

$w_{\mathrm{k,e,F}} = -0.98\mathrm{kN}/m^2$

$w_{\mathrm{k,e,G}} = -0.79\mathrm{kN}/m^2$

$w_{\mathrm{k,e,H}} = -0.43\mathrm{kN}/m^2$

$w_{\mathrm{k,e,I}} = -0.36\mathrm{kN}/m^2$

In the case of the transversal wind, the value of the wind load on the roof is computed below:

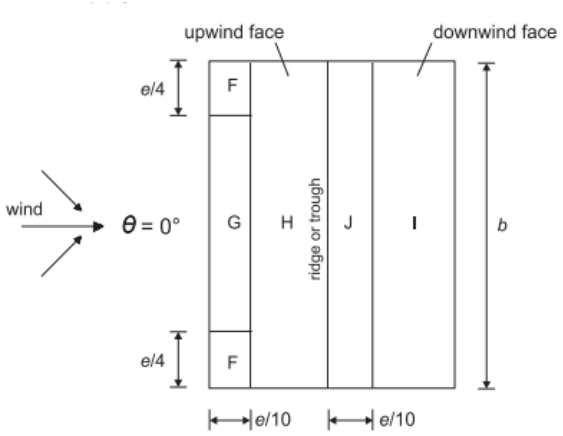

Figure 3.12 Distribution of wind pressure/suction zones on the roof in case of transversal wind [9]

Minimum values:

$c_{pe,10,F} = -1.7$

$c_{pe,10,G} = -1.2$

$c_{pe,10,H} = -0.6$

$c_{pe,10,I} = -0.6$

$c_{pe,10,J} = -0.6$

$w_{k,e,F} = -1.04 kN/m^2$

$w_{k,e,G} = -0.73 kN/m^2$

$w_{k,e,H} = -0.37 kN/m^2$

$w_{k,e,I} = -0.37 kN/m^2$

$w_{k,e,J} = -0.37 kN/m^2$

Maximum values:

$c_{pe,10,F} = 0$

$c_{pe,10,G} = 0$

$c_{pe,10,H} = 0$

$c_{pe,10,I} = -0.6$

$c_{pe,10,J} = 0.2$

$w_{k,e,F} = 0 kN/m^2$

$w_{k,e,G} = 0 kN/m^2$

$w_{k,e,H} = 0 kN/m^2$

$w_{k,e,I} = -0.37 kN/m^2$

$w_{\mathrm{k,e,J}} = 0.12\mathrm{kN}/m^2$

4 cases need to be considered for the transversal wind on the roof where the largest or smallest values of all areas F, G and H are combined with the largest or smallest values in areas I and J. No mixing of positive and negative values is allowed on the same face [9].

3.3.5 Seismic load

The seismic load was computed according to P100-1-2013:

$a_g = 0.2\mathrm{g}$ (for Timisoara)

$T_C = 0.7\mathrm{s}$ (for Timisoara)

$\gamma_{I,e} = 1$ (importance Class III)

The elastic response spectrum is presented in Figure 3.13.

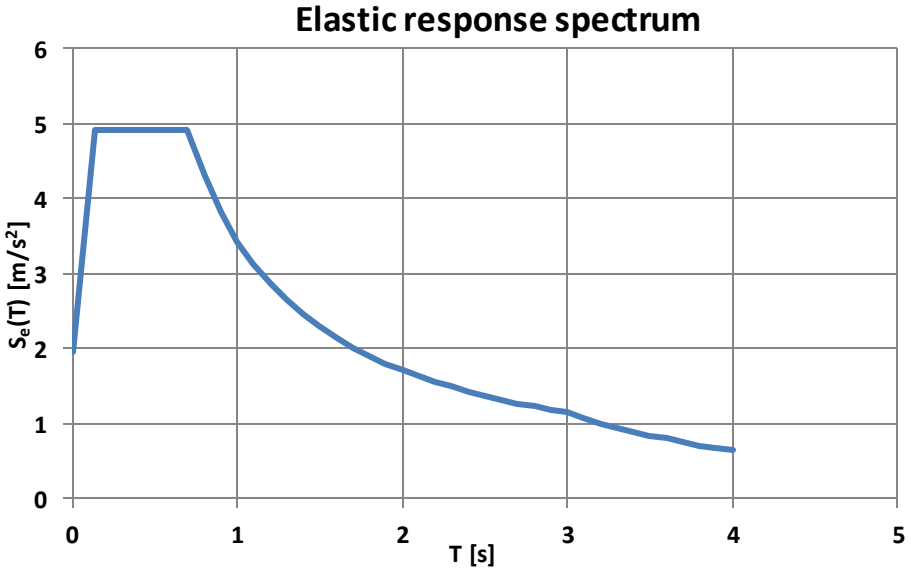

Figure 3.13 Elastic response spectrum for Timisoara

3.3.6 Load combinations

The load combinations were made according to CR 0-2012.

Table 3.1 Values of ψ factors

Load case	ψ_0	ψ_2
Live load (Q)	0.7	0
Snow load (S)	0.7	0.4
Wind load (W)	0.7	0

G – characteristic value of the dead load

Q - characteristic value of the live load

S_u - characteristic value of the undrifted snow load

S_d - characteristic value of the drifted snow load

WL - characteristic value of the longitudinal wind load

WT_MM - characteristic value of the transversal wind load, maximum values for F, G and H, maximum values for I and J

WT_Mm - characteristic value of the transversal wind load, maximum values for F, G and H, minimum values for I and J

WT_mM - characteristic value of the transversal wind load, minimum values for F, G and H, maximum values for I and J

WT_mm - characteristic value of the transversal wind load, minimum values for F, G and H, minimum values for I and J

A – characteristic values of the seismic load

I – design value of the global imperfections

Table 3.2 Load combinations in the fundamental design situation for the Ultimate Limit State

ULS1	1.35G+1.5Q+I
ULS2	1.35G+1.5S_u+I
ULS3	1.35G+1.5S_d+I
ULS4	1.35G+1.5WL+I
ULS5	1.35G+1.5WT_MM+I
ULS6	1.35G+1.5WT_Mm+I
ULS7	1.35G+1.5WT_mM+I
ULS8	1.35G+1.5WT_mm+I
ULS9	1.35G+1.5Q+1.05S_u+I
ULS10	1.35G+1.5Q+1.05S_d+I
ULS11	1.35G+1.5Q+1.05WL+I
ULS12	1.35G+1.5Q+1.05WT_MM+I
ULS13	1.35G+1.5Q+1.05WT_Mm+I
ULS14	1.35G+1.5Q+1.05WT_mM+I
ULS15	1.35G+1.5Q+1.05WT_mm+I

ULS16	1.35G+1.5S_u+1.05Q+I
ULS17	1.35G+1.5S_u+1.05WL+I
ULS18	1.35G+1.5S_u+1.05WT_MM+I
ULS19	1.35G+1.5S_u+1.05WT_Mm+I
ULS20	1.35G+1.5S_u+1.05WT_mM+I
ULS21	1.35G+1.5S_u+1.05WT_mm+I
ULS22	1.35G+1.5S_d+1.05Q+I
ULS23	1.35G+1.5S_d+1.05WL+I
ULS24	1.35G+1.5S_d+1.05WT_MM+I
ULS25	1.35G+1.5S_d+1.05WT_Mm+I
ULS26	1.35G+1.5S_d+1.05WT_mM+I
ULS27	1.35G+1.5S_d+1.05WT_mm+I
ULS28	1.35G+1.5WL+1.05Q+I
ULS29	1.35G+1.5WL+1.05S_u+I
ULS30	1.35G+1.5WL+1.05S_d+I
ULS31	1.35G+1.5WT_MM+1.05Q+I
ULS32	1.35G+1.5WT_MM+1.05S_u+I
ULS33	1.35G+1.5WT_MM+1.05S_d+I
ULS34	1.35G+1.5WT_Mm+1.05Q+I
ULS35	1.35G+1.5WT_Mm+1.05S_u+I
ULS36	1.35G+1.5WT_Mm+1.05S_d+I
ULS37	1.35G+1.5WT_mM+1.05Q+I
ULS38	1.35G+1.5WT_mM+1.05S_u+I
ULS39	1.35G+1.5WT_mM+1.05S_d+I
ULS40	1.35G+1.5WT_mm+1.05Q+I
ULS41	1.35G+1.5WT_mm+1.05S_u+I

ULS42	1.35G+1.5WT_mm+1.05S_d+I
ULS43	1.35G+1.5Q+1.05S_u+1.05WL+I
ULS44	1.35G+1.5Q+1.05S_u+1.05WT_MM+I
ULS45	1.35G+1.5Q+1.05S_u+1.05WT_Mm+I
ULS46	1.35G+1.5Q+1.05S_u+1.05WT_mM+I
ULS47	1.35G+1.5Q+1.05S_u+1.05WT_mm+I
ULS48	1.35G+1.5Q+1.05S_d+1.05WL+I
ULS49	1.35G+1.5Q+1.05S_d+1.05WT_MM+I
ULS50	1.35G+1.5Q+1.05S_d+1.05WT_Mm+I
ULS51	1.35G+1.5Q+1.05S_d+1.05WT_mM+I
ULS52	1.35G+1.5Q+1.05S_d+1.05WT_mm+I
ULS53	1.35G+1.5S_u+1.05Q+1.05WL+I
ULS54	1.35G+1.5S_u+1.05Q+1.05WT_MM+I
ULS55	1.35G+1.5S_u+1.05Q+1.05WT_Mm+I
ULS56	1.35G+1.5S_u+1.05Q+1.05WT_mM+I
ULS57	1.35G+1.5S_u+1.05Q+1.05WT_mm+I
ULS58	1.35G+1.5S_d+1.05Q+1.05WL+I
ULS59	1.35G+1.5S_d+1.05Q+1.05WT_MM+I
ULS60	1.35G+1.5S_d+1.05Q+1.05WT_Mm+I
ULS61	1.35G+1.5S_d+1.05Q+1.05WT_mM+I
ULS62	1.35G+1.5S_d+1.05Q+1.05WT_mm+I
ULS63	1.35G+1.5WL+1.05Q+1.05S_u+I
ULS64	1.35G+1.5WL+1.05Q+1.05S_d+I
ULS65	1.35G+1.5WT_MM+1.05Q+1.05S_u+I
ULS66	1.35G+1.5WT_MM+1.05Q+1.05S_d+I
ULS67	1.35G+1.5WT_Mm+1.05Q+1.05S_u+I

ULS68	1.35G+1.5WT_Mm+1.05Q+1.05S_d+I
ULS69	1.35G+1.5WT_mM+1.05Q+1.05S_u+I
ULS70	1.35G+1.5WT_mM+1.05Q+1.05S_d+I
ULS71	1.35G+1.5WT_mm+1.05Q+1.05S_u+I
ULS72	1.35G+1.5WT_mm+1.05Q+1.05S_d+I
ULS73	G+1.5WL+I
ULS74	G+1.5WT_MM+I
ULS75	G+1.5WT_Mm+I
ULS76	G+1.5WT_mM+I
ULS77	G+1.5WT_mm+I

Table 3.3 Load combinations in the fundamental design situation for the Serviceability Limit State

SLS1	G+Q+I
SLS2	G+S_u+I
SLS3	G+S_d+I
SLS4	G+WL+I
SLS5	G+WT_MM+I
SLS6	G+WT_Mm+I
SLS7	G+WT_mM+I
SLS8	G+WT_mm+I
SLS9	G+Q+0.7S_u+I
SLS10	G+Q+0.7S_d+I
SLS11	G+Q+0.7WL+I
SLS12	G+Q+0.7WT_MM+I
SLS13	G+Q+0.7WT_Mm+I
SLS14	G+Q+0.7WT_mM+I
SLS15	G+Q+0.7WT_mm+I

SLS16	$G+S_u+0.7Q+I$
SLS17	$G+S_u+0.7WL+I$
SLS18	$G+S_u+0.7WT\_MM+I$
SLS19	$G+S_u+0.7WT\_Mm+I$
SLS20	$G+S_u+0.7WT\_mM+I$
SLS21	$G+S_u+0.7WT\_mm+I$
SLS22	$G+S_d+0.7Q+I$
SLS23	$G+S_d+0.7WL+I$
SLS24	$G+S_d+0.7WT\_MM+I$
SLS25	$G+S_d+0.7WT\_Mm+I$
SLS26	$G+S_d+0.7WT\_mM+I$
SLS27	$G+S_d+0.7WT\_mm+I$
SLS28	$G+WL+0.7Q+I$
SLS29	$G+WL+0.7S_u+I$
SLS30	$G+WL+0.7S_d+I$
SLS31	$G+WT\_MM+0.7Q+I$
SLS32	$G+WT\_MM+0.7S_u+I$
SLS33	$G+WT\_MM+0.7S_d+I$
SLS34	$G+WT\_Mm+0.7Q+I$
SLS35	$G+WT\_Mm+0.7S_u+I$
SLS36	$G+WT\_Mm+0.7S_d+I$
SLS37	$G+WT\_mM+0.7Q+I$
SLS38	$G+WT\_mM+0.7S_u+I$
SLS39	$G+WT\_mM+0.7S_d+I$
SLS40	$G+WT\_mm+0.7Q+I$
SLS41	$G+WT\_mm+0.7S_u+I$

SLS42	G+WT_mm+0.7S_d+I
SLS43	G+Q+0.7S_u+0.7WL+I
SLS44	G+Q+0.7S_u+0.7WT_MM+I
SLS45	G+Q+0.7S_u+0.7WT_Mm+I
SLS46	G+Q+0.7S_u+0.7WT_mM+I
SLS47	G+Q+0.7S_u+0.7WT_mm+I
SLS48	G+Q+0.7S_d+0.7WL+I
SLS49	G+Q+0.7S_d+0.7WT_MM+I
SLS50	G+Q+0.7S_d+0.7WT_Mm+I
SLS51	G+Q+0.7S_d+0.7WT_mM+I
SLS52	G+Q+0.7S_d+0.7WT_mm+I
SLS53	G+S_u+0.7Q+0.7WL+I
SLS54	G+S_u+0.7Q+0.7WT_MM+I
SLS55	G+S_u+0.7Q+0.7WT_Mm+I
SLS56	G+S_u+0.7Q+0.7WT_mM+I
SLS57	G+S_u+0.7Q+0.7WT_mm+I
SLS58	G+S_d+0.7Q+0.7WL+I
SLS59	G+S_d+0.7Q+0.7WT_MM+I
SLS60	G+S_d+0.7Q+0.7WT_Mm+I
SLS61	G+S_d+0.7Q+0.7WT_mM+I
SLS62	G+S_d+0.7Q+0.7WT_mm+I
SLS63	G+WL+0.7Q+0.7S_u+I
SLS64	G+WL+0.7Q+0.7S_d+I
SLS65	G+WT_MM+0.7Q+0.7S_u+I
SLS66	G+WT_MM+0.7Q+0.7S_d+I
SLS67	G+WT_Mm+0.7Q+0.7S_u+I

SLS68	G+WT_Mm+0.7Q+0.7S_d+I
SLS69	G+WT_mM+0.7Q+0.7S_u+I
SLS70	G+WT_mM+0.7Q+0.7S_d+I
SLS71	G+WT_mm+0.7Q+0.7S_u+I
SLS72	G+WT_mm+0.7Q+0.7S_d+I

Load combination in the seismic design situation

G+0.4S_d+A+I

3.4 Global analysis of the structure

The structural analysis was performed using 2D models. The 2D model of the transversal frame is presented in Figure 3.14.

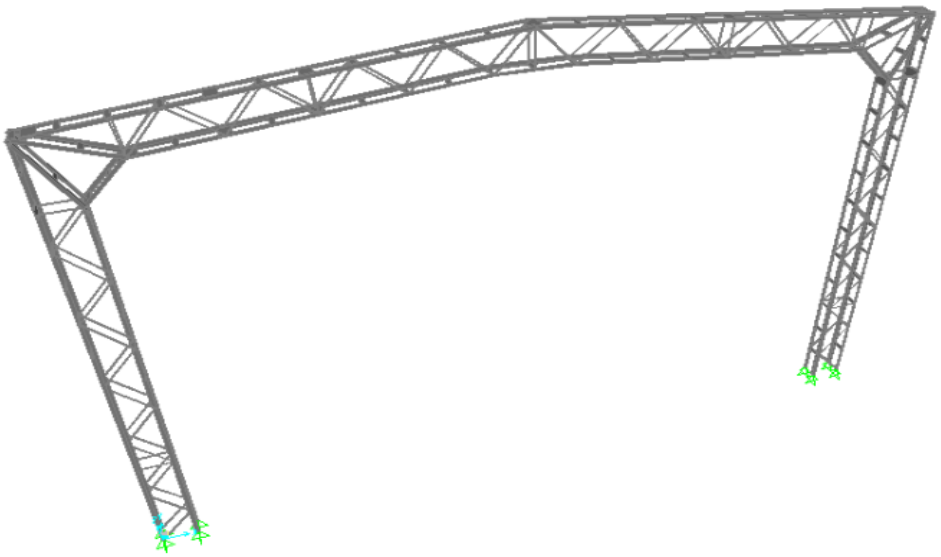

Figure 3.14 2D model of the transversal frame in the initial state

The seismic load is determined by a modal response spectrum analysis. The value of the behavior factor (q) is 1. The seismic masses are considered according to the load combination in the seismic design situation. The sum of the effective modal masses of the considered modes of vibration is greater than 90% of the total seismic mass.

3.4.1 Global imperfections

The global imperfections are taken into account by equivalent horizontal forces.

$\phi_0 = 1/200 = 0.005$

$h = 7.55\text{m}$

$$\alpha_h = \frac{2}{\sqrt{h}} = 0.728 \ (0.667 < \alpha_h < 1 \ is \ fulfilled)$$

$$m = 2$$

$$\alpha_m = \sqrt{0.5\left(1 + \frac{1}{m}\right)} = 0.866$$

$$\phi = \phi_0 \alpha_h \alpha_m = 0.00315$$

$$V_{Ed} = 389.66kN \ (total \ design \ vertical \ load)$$

$$H = \phi V_{Ed} = 1.23kN$$

3.4.2 Global second order effects (for the fundamental design situation)

As $\alpha_{cr} = 14.1 > 10$, global second order effects can be neglected for the fundamental design situation.

3.4.3 Global second order effects (for the seismic design situation)

$$c = 1$$

$$d_{re} = 85.4mm$$

$$d_r = cq\, d_{re} = 85.4mm$$

Table 3.4 Computation of the interstorey drift sensitivity coefficient in the initial state

Level	P_{tot} [kN]	d_r [m]	V_{tot} [kN]	h [m]	θ
1	113.61	0.0854	74.83	7	0.019

As $\theta = 0.019 < 0.1$, global second order effects can be neglected for the seismic design situation.

3.5 Check of the structural members

The transversal frame subjected to the highest loads is the frame in axis 5; therefore, the checks of the structural members are presented for this frame. The check of the girder top angles is presented in the following.

3.5.1 Properties and partial safety factors of the material

$$E = 210000N/mm^2$$

$$\gamma_{M0} = \gamma_{M1} = 1 \ (for \ the \ fundamental \ design \ situation)$$

$$\gamma_{M0} = \gamma_{M1} = 1.1 \ (for \ the \ seismic \ design \ situation)$$

$$\gamma_{M2} = 1.25$$

3.5.2 Properties of the cross-section

The angles are L45x45x5.

$b = h = 45mm$

$t = 5mm$

$A = 430mm^2$

$I_y = I_z = 7.84cm^4$

3.5.3 Value of the internal force

$N_{Ed} = 245.35kN\ (compressive)$

3.5.4 Classification of the cross-section

The cross-section is in compression.

$\varepsilon = 1\ for\ f_y = 235N/mm^2$

$h/t = 9 < 15 = 15\varepsilon$

$$\frac{b+h}{2t} = 9 < 11.5 = 11.5\varepsilon$$

Therefore, the cross-section is class 3.

3.5.5 Resistance of the cross-section

$$N_{c,Rd} = \frac{Af_y}{\gamma_{M0}} = 101.05kN$$

The check:

$$\frac{N_{Ed}}{N_{c,Rd}} = 2.428 > 1 - NOT\ OK$$

3.5.6 Resistance of the member (buckling resistance)

Buckling about yy

$L_{cr,y} = 1.051m$

$$N_{cr,y} = \pi^2 \frac{\mathrm{EI_y}}{\mathrm{L_{cr,y}^2}} = 147.11kN$$

$$\bar{\lambda}_\mathrm{y} = \sqrt{\frac{\mathrm{Af_y}}{\mathrm{N_{cr,y}}}} = 0.829$$

$\alpha_y = 0.34 - buckling\ curve\ b$

$$\Phi_y = 0.5\left[1 + \alpha_y\left(\bar{\lambda}_\mathrm{y} - 0.2\right) + \bar{\lambda}_y^2\right] = 0.951$$

$$\chi_\mathrm{y} = \frac{1}{\Phi_\mathrm{y} + \sqrt{\Phi_\mathrm{y}^2 - \bar{\lambda}_\mathrm{y}^2}} = 0.706 < 1$$

$$N_{by,Rd} = \frac{\chi_\mathrm{y} Af_y}{\gamma_{M1}} = 71.34kN$$

The check:

$$\frac{N_{Ed}}{N_{by,Rd}} = 3.439 > 1 - NOT\ OK$$

Buckling about zz

$$L_{cr,z} = 1.051m$$

$$N_{cr,z} = \pi^2 \frac{\mathrm{EI_z}}{\mathrm{L_{cr,z}^2}} = 147.11\mathrm{kN}$$

$$\bar{\lambda}_z = \sqrt{\frac{\mathrm{Af_y}}{\mathrm{N_{cr,z}}}} = 0.829$$

$$\alpha_z = 0.34 - buckling\ curve\ b$$

$$\Phi_z = 0.5\left[1 + \alpha_z\left(\bar{\lambda}_z - 0.2\right) + \bar{\lambda}_z^2\right] = 0.951$$

$$\chi_z = \frac{1}{\Phi_z + \sqrt{\Phi_z^2 - \bar{\lambda}_z^2}} = 0.706 < 1$$

$$N_{bz,Rd} = \frac{\chi_z A f_y}{\gamma_{M1}} = 71.34kN$$

The check:

$$\frac{N_{Ed}}{N_{bz,Rd}} = 3.439 > 1 - NOT\ OK$$

The checks of all the elements are summarized below:

$Check\ of\ the\ girder\ top\ angles$: $N_{Ed}/N_{b,Rd} = 3.439 > 1$

$Check\ of\ the\ girder\ bottom\ angles$: $N_{Ed}/N_{b,Rd} = 2.103 > 1$

$Check\ of\ the\ column\ angles$: $N_{Ed}/N_{b,Rd} = 3.192 > 1$

$Check\ of\ the\ column\ diagonals\ (\phi 16)$: $N_{Ed}/N_{b,Rd} = 4.018 > 1$

$Check\ of\ the\ column\ diagonals\ (\phi 20)$: $N_{Ed}/N_{b,Rd} = 1.577 > 1$

$Check\ of\ the\ girder\ diagonals\ (\phi 16)$: $N_{Ed}/N_{b,Rd} = 10.232 > 1$

$Check\ of\ the\ girder\ diagonals\ (\phi 20)$: $N_{Ed}/N_{b,Rd} = 4.507 > 1$

$Check\ of\ the\ angles\ in\ the\ node\ region$: $N_{Ed}/NN_{b,Rd} = 2.352 > 1$

Therefore, the bearing capacity of all the structural elements is exceeded.

3.6 Evaluation of the girder-to-column node

In order to determine the bearing capacity of the girder-to-column node, a GMNIA was performed. The numerical model is presented in Figure 3.15.

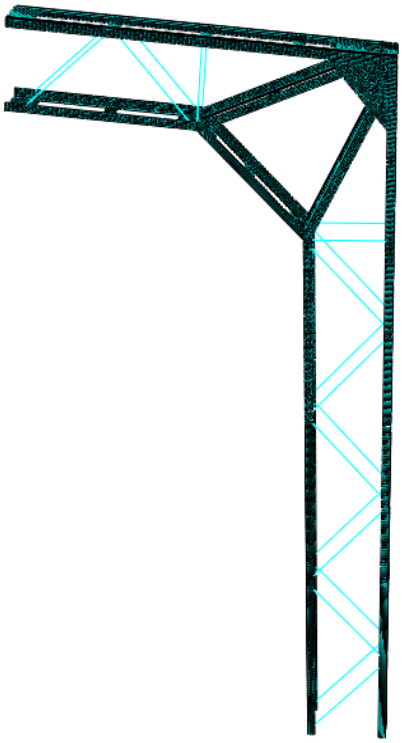

Figure 3.15 Numerical model of the girder-to-column node in the initial state

5 different models were considered (1 model without imperfections and 4 models with different cases of imperfections) in order to determine the most unfavorable situation. The imperfections are applied by first performing an eigen buckling analysis. Following the buckling analysis, it resulted that the eigen buckling modes are given by the flexural buckling of the diagonals (each eigen buckling mode represents either the in-plane or out-of-plane flexural buckling of a pair of diagonals). The shape of the imperfections is applied according to the considered buckling mode with the amplitude e_0 computed according to Eurocode 3-1-1 (See Figure 3.16).

Buckling curve according to Table 6.2	elastic analysis e_0 / L	plastic analysis e_0 / L
a_0	1 / 350	1 / 300
a	1 / 300	1 / 250
b	1 / 250	1 / 200
c	1 / 200	1 / 150
d	1 / 150	1 / 100

Figure 3.16 Design value of the imperfection [10]

The imperfection study is presented in Figure 3.17. The number in the name of each model represents the eigen buckling mode according to which the imperfections are applied (in the case of "Imp 5", the imperfections are applied according to the fifth buckling mode).

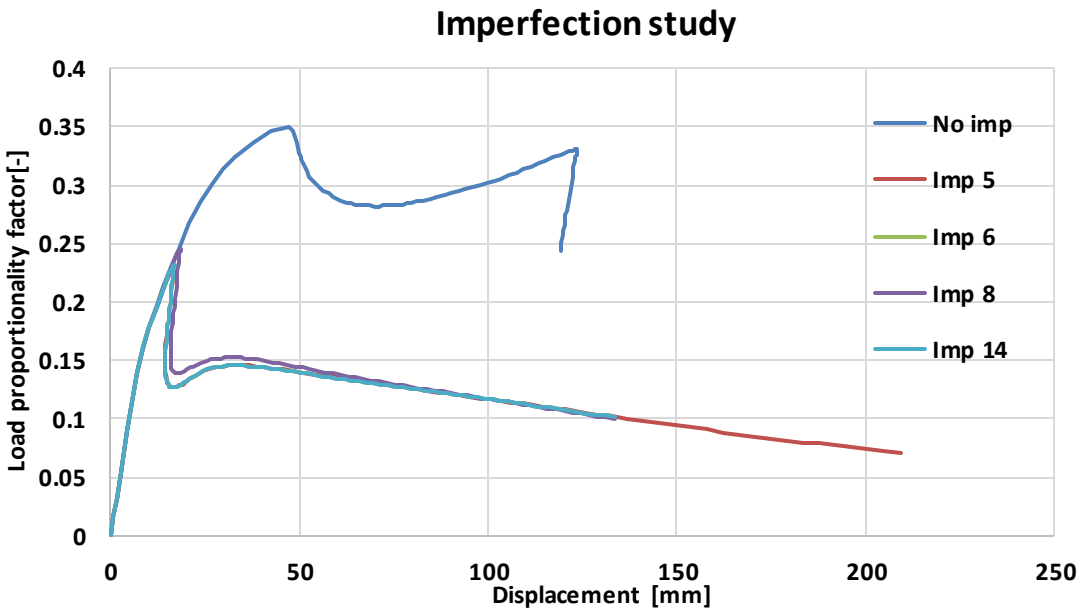

Figure 3.17 Imperfection study for the node in the initial state

The most unfavorable situation is in the case when the imperfections are applied according to the fifth buckling mode. The results are further presented for this case.

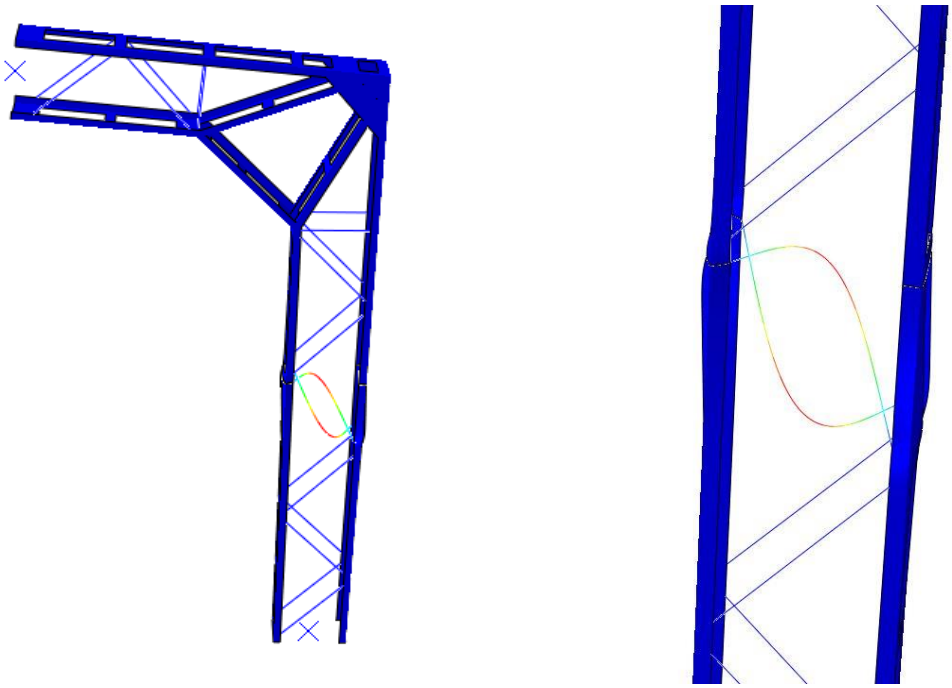

(a) General view of the node *(b) Close-up of the region where the buckling occurs*

Figure 3.18 The fifth buckling mode of the node in the initial state

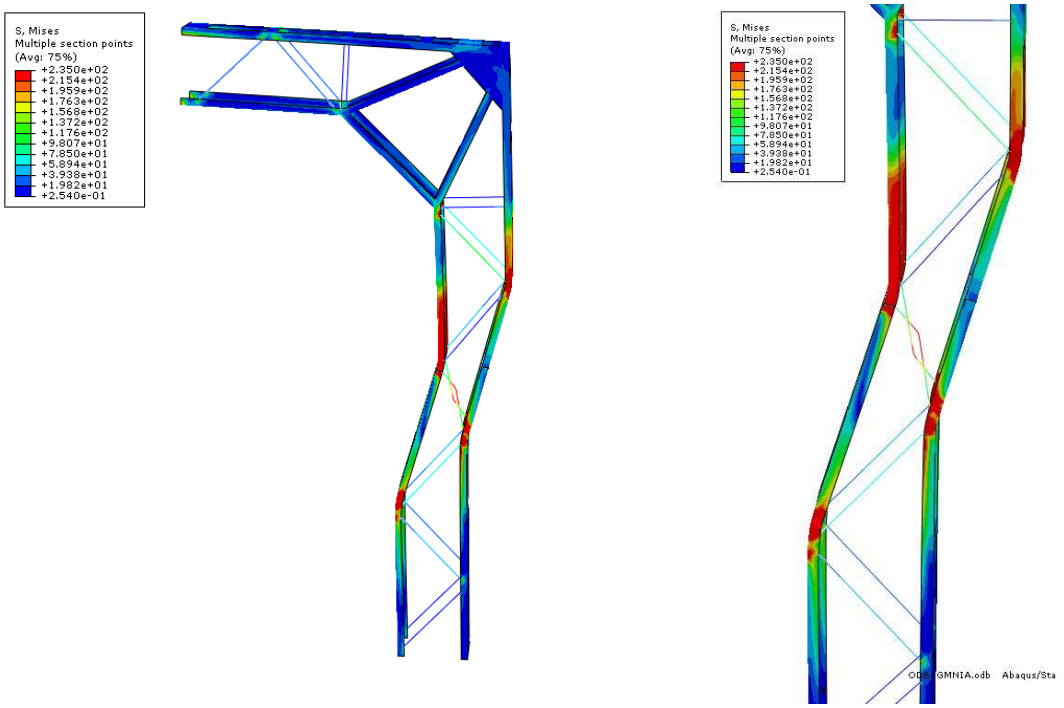

(a) General view of the node *(b) Close-up of the region where the failure occurs*

Figure 3.19 The distribution of von Mises stresses and the deformed shape of the node in the initial state

The failure of the node occurs due to the out-of-plane flexural buckling of the column diagonals, which leads to the formation of a mechanism. The same failure mechanism was observed in case of the damaged girders after the September 2017 storm (See Paragraph 2.3).

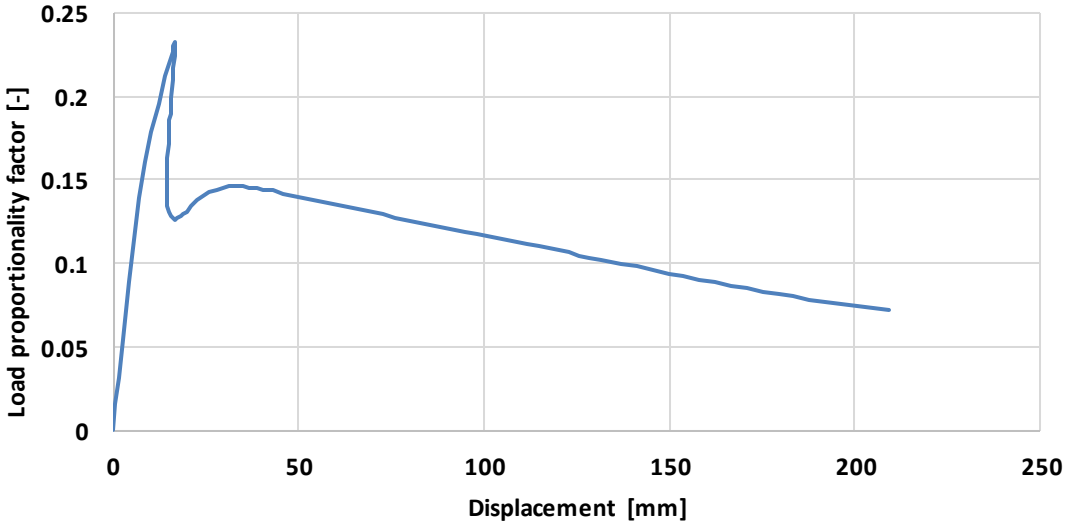

Figure 3.20 Load proportionality factor of the node in the initial state

As the value of the Load Proportionality Factor is 0.23, the bearing capacity of the node is exceeded.

4 PARTIAL REHABILITATION OF THE STRUCTURE AFTER THE STORM

After the September 2017 storm, a partial rehabilitation of the damaged frames was performed in order to restore their initial bearing capacity and to ensure the structural safety in the case of the normal use of the structure (no snow load acting on the structure). The rehabilitation solution is described in Paragraph 4.1.

4.1 The partial rehabilitation solution

The partial rehabilitation of the frames from axes 4 and 5 consists of welding steel plates in the regions where deformations occurred (the nodes in which cracks occurred in the welds, as well as the adjacent nodes in which the weld did not fail) in order to ensure the continuity of the angles. Also, the buckled diagonals will be replaced with new ones. The steel plates have a thickness of 10mm and the new diagonals are angles with the cross-section of L45x45x5. Both the steel plates and the angles are made from S235 steel.

A sketch of the right-hand side of the girder from the frame in axis 4, with the partial rehabilitation solution, is presented in Figure 4.1.

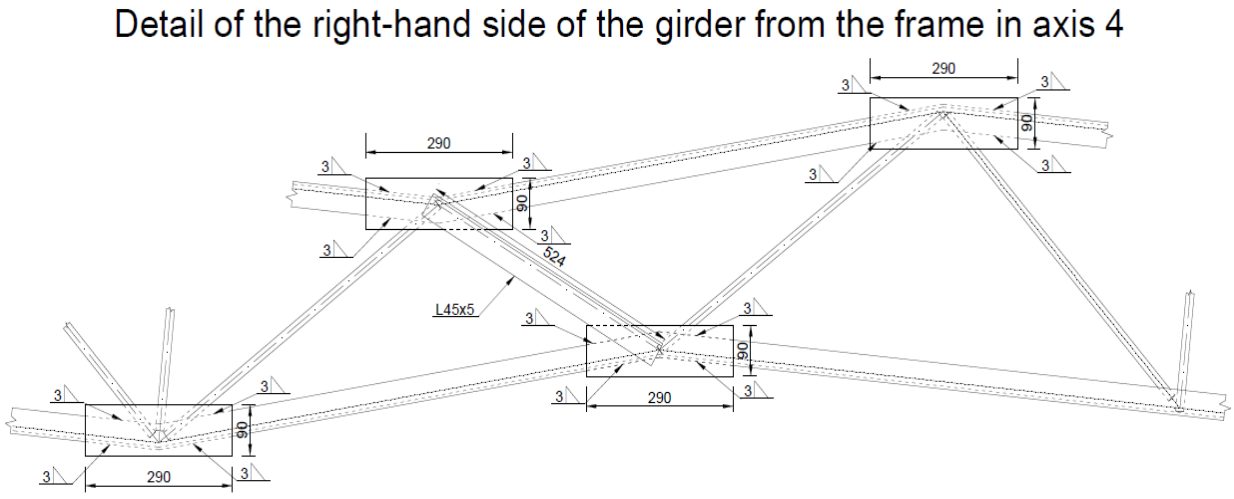

Figure 4.1 Sketch of the partial rehabilitation solution

The right-hand side of the girder from the frame in axis 4, with the applied partial rehabilitation solution, is presented in Figure 4.2.

Figure 4.2 The girder from the frame in axis 4 after the partial rehabilitation

4.2 Design of the welds of the steel plates

The steel plates are welded to the angles both at the top and at the bottom. The force to which the weld needs to be designed is given by the design axial resistance of the angle. However, there is an eccentricity between the centroid of the angle and the centroid of the weld. The additional force due to this eccentricity needs to be taken into account.

$$N_{Ed} = \frac{Af_y}{\gamma_{M0}} = 101.05kN - design\ axial\ resistance\ of\ the\ angle$$

$$b = 45mm - width\ of\ the\ angle$$

$$e_1 = 12.8mm - distance\ from\ the\ centroid\ of\ the\ angle\ to\ the\ bottom\ of\ the\ angle$$

$$g_w = 22.5mm - distance\ from\ the\ centroid\ of\ the\ weld\ to\ the\ bottom\ of\ the\ angle$$

$$d_1 = g_w - e_1 - eccentricity\ between\ the\ angle\ centroid\ and\ the\ weld\ centroid$$

$$d_1 = 9.7mm$$

$$M_W = N_{Ed} \cdot d_1 = 0.98kNm - moment\ due\ to\ the\ eccentricity$$

$$F_{Ed} = \frac{N_{Ed}}{2} + \frac{M_W}{b} = 72.31kN - force\ for\ the\ design\ of\ one\ weld\ (top\ or\ bottom)$$

$$f_u = 360N/mm^2\ (for\ S235)$$

$$\beta_w = 0.8\ (for\ S235)$$

$$f_{vw,d} = \frac{f_u}{\sqrt{3} \cdot \beta_w \cdot \gamma_{M2}} = 207.85N/mm^2$$

$$a = a_{min} = 3mm - thickness\ of\ the\ weld$$

$$F_{w,Rd} = f_{vw,d} \cdot a = 623.55N/mm$$

$F_{w,Ed} = F_{Ed}/l \leq F_{w,Rd} \Rightarrow l \geq F_{Ed}/F_{w,Rd} = 116mm$

$l = 145mm > 30mm = l_{min} = \max(30,6a) - \ length\ of\ one\ weld$

$F_{w,Ed} = F_{Ed}/l = 498.69N/mm$

The check:

$$\frac{F_{w,Ed}}{F_{w,Rd}} = 0.8 < 1 - OK$$

4.3 Global analysis of the structure

The 2D model of the deformed transversal frame in axis 4 is presented in Figure 4.3 (buckled diagonals are replaced with new ones and the steel plates are provided in the regions where deformations occurred). The crack in the weld is modeled by a discontinuity in the angles. A similar model was used for the analysis of the frame in axis 5.

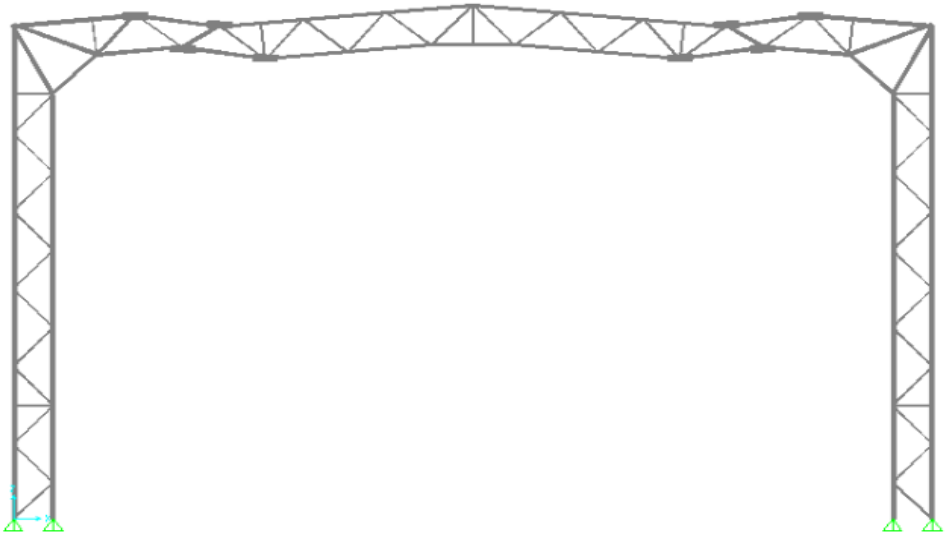

Figure 4.3 2D model of the transversal frame in axis 4, after the storm, with the partial rehabilitation solution

The seismic analysis is performed as in the case of the frame in the initial state. The global imperfections are taken into account by considering the equivalent horizontal force computed in Paragraph 3.4.1. Global second order effects can be neglected (for both the fundamental and the seismic design situations).

4.4 Check of the structural elements

The checks of all the elements are summarized below for the frame in axis 5 (most unfavorable situation).

$Check\ of\ the\ angles\ replacing\ the\ buckled\ diagonals$: $N_{Ed}/N_{b,Rd} = 1.191 > 1$

$Check\ of\ the\ girder\ top\ angles$: $N_{Ed}/N_{b,Rd} = 3.448 > 1$

$Check\ of\ the\ girder\ bottom\ angles$: $N_{Ed}/N_{b,Rd} = 2.108 > 1$

$Check\ of\ the\ column\ angles$: $N_{Ed}/N_{b,Rd} = 3.19 > 1$

$Check\ of\ the\ column\ diagonals\ (\phi 16)$: $N_{Ed}/N_{b,Rd} = 4.012 > 1$

$Check\ of\ the\ column\ diagonals\ (\phi 20)$: $N_{Ed}/N_{b,Rd} = 1.574 > 1$

$Check\ of\ the\ girder\ diagonals\ (\phi 16)$: $N_{Ed}/N_{b,Rd} = 3.37 > 1$

$Check\ of\ the\ girder\ diagonals\ (\phi 20)$: $N_{Ed}/N_{b,Rd} = 4.51 > 1$

$Check\ of\ the\ angles\ in\ the\ node\ region$: $N_{Ed}/N_{b,Rd} = 2.351 > 1$

It can be observed that the values of these checks are similar to the values of the checks in case of the initial undeformed structure. Therefore, the bearing capacity of the frame is restored following the partial rehabilitation, but is still exceeded (the checks are presented only for the frame in axis 5; the observation is valid also for the frame in axis 4).

However, in the case of the normal use of the structure (no snow load acting on the structure), the structural safety is ensured. The checks of all the elements are summarized below for the frame in axis 5, in the case when the snow load is not acting on the structure:

$Check\ of\ the\ angles\ replacing\ the\ buckled\ diagonals$: $N_{Ed}/N_{b,Rd} = 0.254 < 1$

$Check\ of\ the\ girder\ top\ angles$: $N_{Ed}/N_{b,Rd} = 0.766 < 1$

$Check\ of\ the\ girder\ bottom\ angles$: $N_{Ed}/N_{b,Rd} = 0.477 < 1$

$Check\ of\ the\ column\ angles$: $N_{Ed}/N_{b,Rd} = 0.739 < 1$

$Check\ of\ the\ column\ diagonals\ (\phi 16)$: $N_{Ed}/N_{b,Rd} = 0.977 < 1$

$Check\ of\ the\ column\ diagonals\ (\phi 20)$: $N_{Ed}/N_{b,Rd} = 0.387 < 1$

$Check\ of\ the\ girder\ diagonals\ (\phi 16)$: $N_{Ed}/N_{b,Rd} = 0.766 < 1$

$Check\ of\ the\ girder\ diagonals\ (\phi 20)$: $N_{Ed}/N_{b,Rd} = 0.992 < 1$

$Check\ of\ the\ angles\ in\ the\ node\ region$: $N_{Ed}/N_{b,Rd} = 0.543 < 1$

5 FINAL REHABILITATION OF THE STRUCTURE

As previously presented in Paragraphs 3.5, 3.6 and 4.4, the bearing capacity of the structure is greatly exceeded. Consequently, a structural upgrade (rehabilitation) is considered in order to extend the service life of the structure (therefore reusing it). The rehabilitation solution is described in Paragraph 5.1.

The rehabilitation solution was validated by following the steps presented in Figure 5.1.

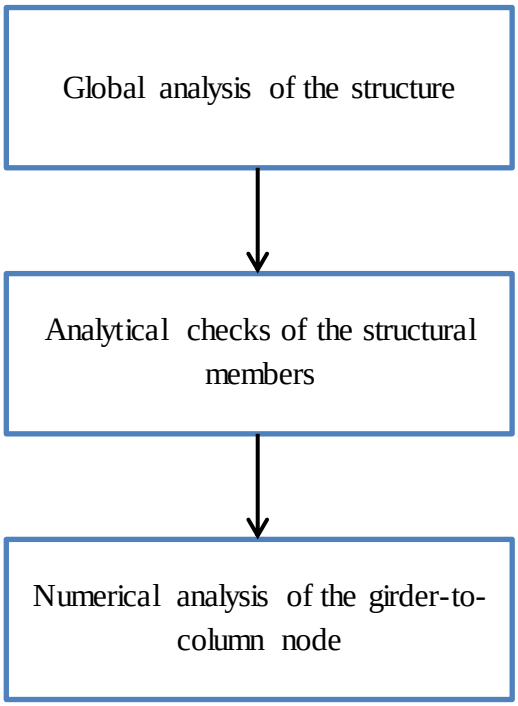

Figure 5.1 Flow chart for the validation of the rehabilitation solution

5.1 The final rehabilitation solution

The final rehabilitation solution consists of welding S355 steel plates to the angles of the girder and the column, forming a box section. For the girder, the steel plates have a thickness of 3mm (on all sides). For the column, the steel plates have a thickness of 3mm on the short side, while on the long side they have a thickness of 8mm at the base of the column and 6mm at the top (including the node region). The damaged girders from the frames in axes 4 and 5 will be replaced by girders having the same configuration, made from S355 steel.

The validation of the rehabilitation solution is presented in the following Paragraphs.

5.2 Global analysis of the structure

The most unfavorable situation is in the case of the frame in axis 5. The checks will be presented for this frame.

The 2D model of the transversal frame is presented in Figure 5.2. It is no longer possible to model each element individually due to the fact that, by welding the steel plates to the angles,

the girders and columns will now have a composite cross-section. Therefore, the girders and columns are modelled with their composite cross-section centroid axes.

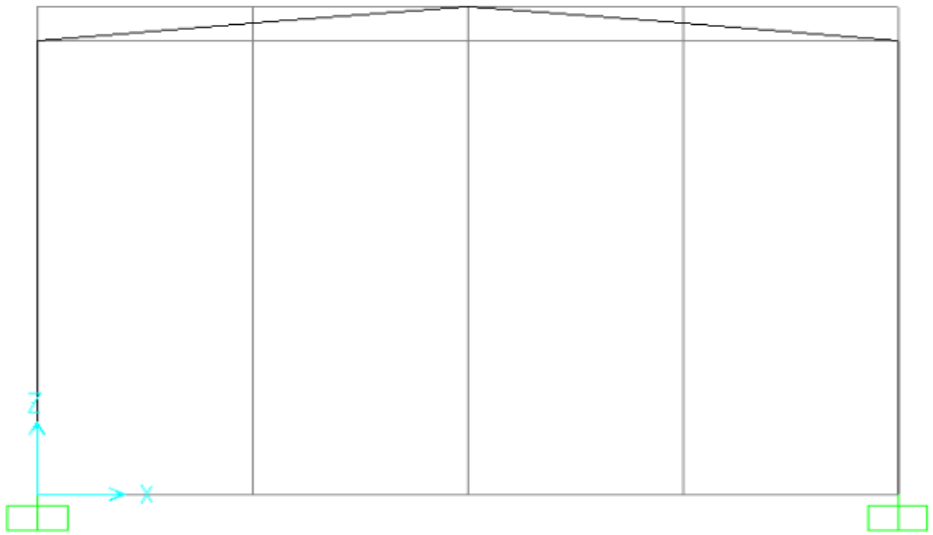

Figure 5.2 2D model of the transversal frame after the final rehabilitation

The seismic load is determined by a modal response spectrum analysis. The value of the behavior factor (q) is 1. The seismic masses are considered according to the load combination in the seismic design situation. The sum of the effective modal masses of the considered modes of vibration is greater than 90% of the total seismic mass.

5.2.1 Global imperfections

The global imperfections are taken into account by considering the equivalent horizontal force computed in Paragraph 3.4.1.

5.2.2 Global second order effects (for the fundamental design situation)

As $\alpha_{cr} = 44.1 > 10$, global second order effects can be neglected for the fundamental design situation.

5.2.3 Global second order effects (for the seismic design situation)

$d_{re} = 28.3mm$

$d_r = cq\, d_{re} = 28.3mm$

Table 5.1 Computation of the interstorey drift sensitivity coefficient after the final rehabilitation

Level	P_{tot} [kN]	d_r [m]	V_{tot} [kN]	h [m]	θ
1	124.41	0.0283	78.86	6.775	0.007

As $\theta = 0.007 < 0.1$, global second order effects can be neglected for the seismic design situation.

5.3 Check of the girder

The cross-section of the girder is presented in Figure 5.3.

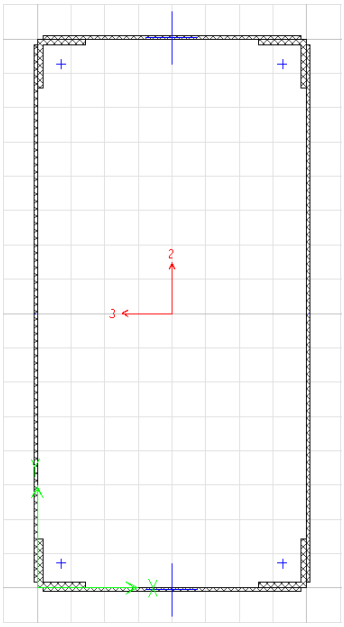

Figure 5.3 Cross-section of the girder after the final rehabilitation

The steel plates have a thickness of 3mm. As mentioned previously, the angles are class 3. However, considering the composite box section, the steel plates are class 4. Therefore, the effective properties (A_{eff} and $W_{eff,y,min}$) of the cross-section need to be determined according to SR EN 1993-1-5. Both the flanges and the webs are internal compression elements.

5.3.1 Determination of A_{eff}

The effective area A_{eff} is determined by considering that the cross-section is subjected to pure compression.

Classification of the web

The web is in pure compression.

$h = 490mm$

$t = 3mm$

$c = h - 2 \cdot 40 = 410mm$

$\varepsilon = 0.81\ for\ S355$

$c/t = 136.67 > 34.02 = 42\varepsilon\ \Rightarrow\ web\ is\ class\ 4$

Classification of the flange

The flange is in pure compression.

$b = 240mm$

$t = 3mm$

$c = b - 2 \cdot 40 = 160mm$

$\varepsilon = 0.81\ for\ S355$

$c/t = 53.33 > 34.02 = 42\varepsilon\ \Rightarrow\ flange\ is\ class\ 4$

Therefore, the cross-section is class 4.

Determination of the effective width of the flange

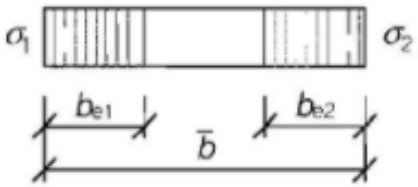

Figure 5.4 Stress distribution in the flange in case of pure compression [11]

$\psi = 1$

$k_\sigma = 4$

$\bar{b} = c = 160mm$

$$\bar{\lambda}_p = \frac{\bar{b}/t}{28.4\varepsilon\sqrt{k_\sigma}} = 1.159 > 0.673 = 0.5 + \sqrt{0.085 - 0.055 \cdot \psi}$$

$$Therefore, \rho = \frac{\bar{\lambda}_p - 0.055 \cdot (3 + \psi)}{\bar{\lambda}_p{}^2} = 0.699 < 1$$

$b_{eff} = \rho \cdot \bar{b} = 111.84mm$

$b_{e1} = b_{e2} = 0.5 \cdot b_{eff} = 55.92mm$

Determination of the effective width of the web

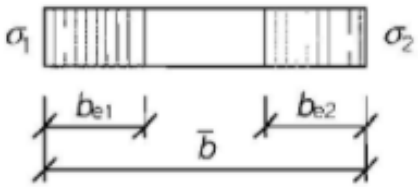

Figure 5.5 Stress distribution in the web in case of pure compression [11]

$\psi = 1$

$k_\sigma = 4$

$\bar{b} = c = 410mm$

$$\bar{\lambda}_p = \frac{\bar{b}/t}{28.4\varepsilon\sqrt{k_\sigma}} = 2.97 > 0.673 = 0.5 + \sqrt{0.085 - 0.055 \cdot \psi}$$

$$Therefore, \rho = \frac{\bar{\lambda}_p - 0.055 \cdot (3 + \psi)}{\bar{\lambda}_p{}^2} = 0.312 < 1$$

$$b_{eff} = \rho \cdot \bar{b} = 127.92mm$$

$$b_{e1} = b_{e2} = 0.5 \cdot b_{eff} = 63.96mm$$

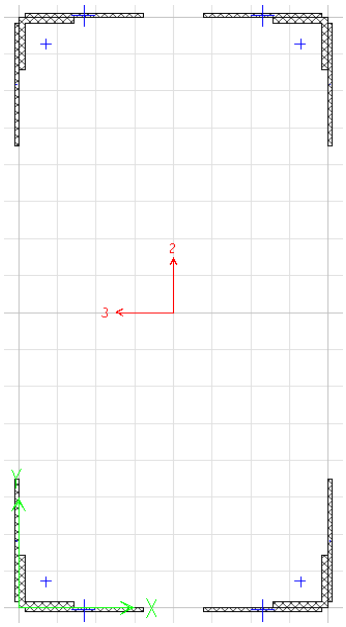

Figure 5.6 Effective cross-section of the girder in case of pure compression

$A_{eff} - effective\ area\ of\ the\ cross - section, considering\ only\ the\ steel\ plates$

$A_{eff} = 2398.56mm^2$

$A = 1720mm^2 \ - \ area\ of\ the\ angles$

The characteristic axial resistance of the cross-section is determined as follows:

$N_{Rk} = A_{eff} \cdot f_{y,p} + A \cdot f_{y,a} = 1462.09kN$

$f_{y,p} - yield\ strength\ of\ the\ steel\ used\ for\ the\ plates$

$f_{y,a} - yield\ strength\ of\ the\ steel\ used\ for\ the\ angles$

$f_{y,p} = 355N/mm^2 \ \ (steel\ plates\ made\ from\ S355\ steel)$

$f_{y,a} = 355N/mm^2$ (as mentioned above, the girders from the frames in axes 4 and 5 are replaced by girders made from S355 steel; for the other girders, $f_{y,a} = 235N/mm^2$)

5.3.2 Determination of $W_{eff,y,min}$

The minimum effective section modulus about the major inertia axis $W_{eff,y,min}$ is determined by considering that the cross-section is subjected only to bending about the major inertia axis.

Classification of the web

The web is in pure bending.

$h = 490mm$

$t = 3mm$

$c = h - 2 \cdot 40 = 410mm$

$\varepsilon = 0.81\ for\ S355$

$c/t = 136.67 > 100.44 = 124\varepsilon\ \Rightarrow\ web\ is\ class\ 4$

Classification of the flange

The flange is in pure compression.

$b = 240mm$

$t = 3mm$

$c = b - 2 \cdot 40 = 160mm$

$\varepsilon = 0.81\ for\ S355$

$c/t = 53.33 > 34.02 = 42\varepsilon\ \Rightarrow\ flange\ is\ class\ 4$

Therefore, the cross-section is class 4.

Determination of the effective width of the flange

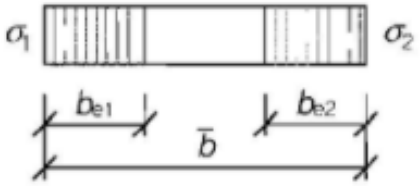

Figure 5.7 Stress distribution in the flange in case of pure bending about the major inertia axis [11]

$\psi = 1$

$k_\sigma = 4$

$\bar{b} = c = 160mm$

$$\bar{\lambda}_p = \frac{\bar{b}/t}{28.4\varepsilon\sqrt{k_\sigma}} = 1.159 > 0.673 = 0.5 + \sqrt{0.085 - 0.055 \cdot \psi}$$

$$Therefore, \rho = \frac{\bar{\lambda}_p - 0.055 \cdot (3 + \psi)}{\bar{\lambda}_p{}^2} = 0.699 < 1$$

$b_{eff} = \rho \cdot \bar{b} = 111.84mm$

$b_{e1} = b_{e2} = 0.5 \cdot b_{eff} = 55.92mm$

Determination of the effective width of the web

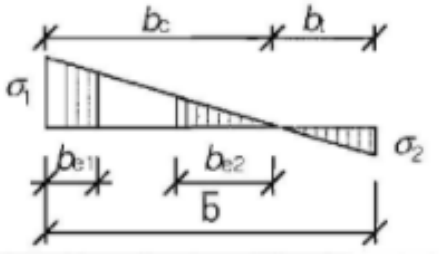

Figure 5.8 Stress distribution in the web in case of pure bending about the major inertia axis [11]

$\psi = -0.942$ (the new position of the neutral axis is determined, accounting for the local buckling of the flange in compression)

$$k_\sigma = 7.81 - 6.29 \cdot \psi + 9.78 \cdot \psi^2 = 22.41$$

$$\bar{b} = c = 410mm$$

$$\bar{\lambda}_p = \frac{\bar{b}/t}{28.4\varepsilon\sqrt{k_\sigma}} = 1.255 > 0.87 = 0.5 + \sqrt{0.085 - 0.055 \cdot \psi}$$

$$Therefore, \rho = \frac{\bar{\lambda}_p - 0.055 \cdot (3 + \psi)}{\bar{\lambda}_p{}^2} = 0.725 < 1$$

$$b_c = \bar{b}/(1 - \psi) = 211.12mm$$

$$b_t = \bar{b} - b_c = 198.88mm$$

$$b_{eff} = \rho \cdot b_c = 153.06mm$$

$$b_{e1} = 0.4 \cdot b_{eff} = 61.22mm$$

$$b_{e2} = 0.6 \cdot b_{eff} = 91.84mm$$

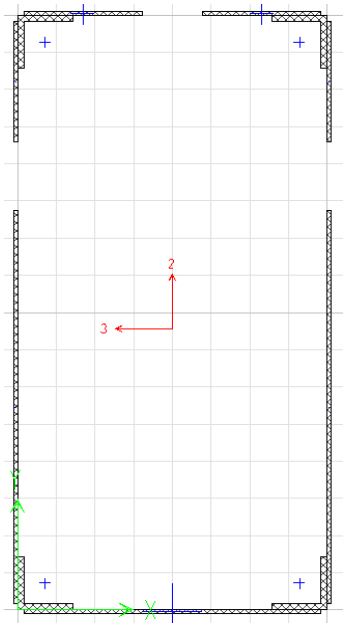

Figure 5.9 Effective cross-section of the girder in case of pure bending about the major inertia axis

$W_{eff,y,min} = 505.34cm^3$ - minimum effective section modulus about the major inertia axis, considering only the steel plates

The characteristic bending resistance moment of the cross-section, about the major inertia axis, is determined as follows:

$M_{y,Rk} = W_{eff,y,min} \cdot f_{y,p} + 2 \cdot A \cdot f_{y,a} \cdot d = 324.23kNm$

$f_{y,p} - yield\ strength\ of\ the\ steel\ used\ for\ the\ plates$

$f_{y,a} - yield\ strength\ of\ the\ steel\ used\ for\ the\ angles$

$A - cross - sectional\ area\ of\ one\ angle$

$d - distance\ between\ the\ centroids\ of\ the\ top\ and\ bottom\ angles$

$f_{y,p} = 355N/mm^2\ (steel\ plates\ made\ from\ S355\ steel)$

$f_{y,a} = 355N/mm^2$ (as mentioned above, the girders from the frames in axes 4 and 5 are replaced by girders made from S355 steel; for the other girders, $f_{y,a} = 235N/mm^2$)

$A = 430mm^2$

$d = 474.4mm$

5.3.3 Values of the internal forces

$N_{Ed} = 72.62kN\ (compressive)$

$V_{z,Ed} = 140.19kN$

$M_{y,Ed} = 253.35kNm$

5.3.4 Resistance of the cross-section

Resistance check to axial force and bending moment about the major inertia axis

The check:

$$\eta_1 = \frac{N_{Ed}}{\frac{N_{Rk}}{\gamma_{M0}}} + \frac{M_{y,Ed} + N_{Ed}e_{y,N}}{\frac{M_{y,Rk}}{\gamma_{M0}}} = 0.831 < 1 - OK$$

$e_{y,N} = 0$ (the cross-section is doubly-symmetrical, no shift of the centroid occurs)

Resistance check to shear buckling

$f_{yw} = 355N/mm^2$

$\varepsilon = 0.81\ for\ f_{yw} = 355N/mm^2$

$\eta = 1.2\ for\ S355$

$h_w = 490mm$

$t_w = 3mm$

$$\frac{h_w}{t_w} = 163.33 > 48.6 = 72 \cdot \frac{\varepsilon}{\eta} => the\ shear\ buckling\ resistance\ must\ be\ checked$$

$$\bar{\lambda}_w = \frac{h_w}{86.4t\varepsilon} = 2.334\ (transverse\ stiffeners\ at\ supports\ only)$$

$$\chi_w = \frac{0.83}{\bar{\lambda}_w} = 0.356\ \left(\bar{\lambda}_w > 1.08, non - rigid\ end\ post\right)$$

$$V_{bw,Rd} = 2 \cdot \frac{\chi_w f_{yw} h_w t}{\sqrt{3}\gamma_{M1}} = 214.52kN\ (contribution\ from\ both\ webs)$$

$$V_{bf,Rd} = 0kN\ (contribution\ from\ flanges\ is\ neglected)$$

$$V_{b,Rd} = V_{bw,Rd} + V_{bf,Rd} = 214.52kN < 723.1kN = 2 \cdot \frac{\eta f_{yw} h_w t}{\sqrt{3}\gamma_{M1}}$$

The check:

$$\eta_3 = \frac{V_{Ed}}{V_{b,Rd}} = 0.654 < 1 - OK$$

$$\bar{\eta}_3 = \frac{V_{Ed}}{V_{bw,Rd}} = 0.654 > 0.5$$

Therefore, the effect of the shear force on the bending resistance needs to be considered.

The check:

$$\bar{\eta}_1 + \left(1 - \frac{M_{f,Rd}}{M_{pl,Rd}}\right)(2\bar{\eta}_3 - 1)^2 = 0.926 < 1 - OK$$

$$\bar{\eta}_1 = \eta_1 = 0.831$$

$$M_{f,Rd} = 0$$

5.3.5 Resistance of the member (buckling resistance)

Buckling about yy

$$L_{cr,y} = 10.5m$$

$$I_{y,b} = 24564.8cm^4 - gross\ moment\ of\ inertia$$

$$N_{cr,y} = \pi^2 \frac{\mathrm{EI_{y,b}}}{\mathrm{L^2_{cr,y}}} = 4618kN$$

$$\bar{\lambda}_y = \sqrt{\frac{N_{Rk}}{\mathrm{N_{cr,y}}}} = 0.563$$

$$\alpha_y = 0.49 - buckling\ curve\ c$$

$$\Phi_y = 0.5\left[1 + \alpha_y\left(\bar{\lambda}_y - 0.2\right) + \bar{\lambda}_y^2\right] = 0.747$$

$$\chi_y = \frac{1}{\Phi_y + \sqrt{\Phi_y^2 - \bar{\lambda}_y^2}} = 0.808 < 1$$

Buckling about zz

$L_{cr,z} = 10.5m$

$I_{z,b} = 7557.5cm^4 \; - gross\ moment\ of\ inertia$

$$N_{cr,z} = \pi^2 \frac{EI_{z,b}}{L_{cr,z}^2} = 1420.75kN$$

$$\bar{\lambda}_z = \sqrt{\frac{N_{Rk}}{N_{cr,z}}} = 1.014$$

$\alpha_z = 0.49 - \ buckling\ curve\ c$

$$\Phi_z = 0.5\left[1 + \alpha_z\left(\bar{\lambda}_z - 0.2\right) + \bar{\lambda}_z^2\right] = 1.214$$

$$\chi_z = \frac{1}{\Phi_z + \sqrt{\Phi_z^2 - \bar{\lambda}_z^2}} = 0.531 < 1$$

Lateral-torsional buckling

As the girder has a box section, it is not susceptible to lateral-torsional buckling. Therefore, $\chi_{LT} = 1$.

Computation of the interaction factors

The interaction factors are computed according to Annex B, Table B.1 (members not susceptible to torsional deformations).

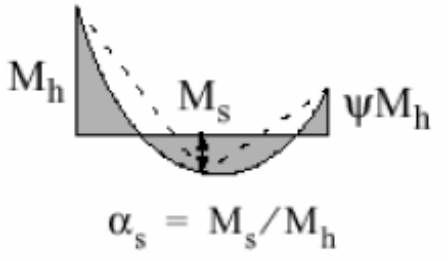

Figure 5.10 Shape of the bending moment diagram on the girder [10]

$M_s = 227.51kNm$

$M_h = -253.35kNm$

$\alpha_s = -0.898$

$\psi M_h = -250.31kNm$

$\psi = 0.988$

$Since\ -1 \le \alpha_s < 0{,}0 \le \psi \le 1, uniform\ loading, non - sway\ buckling\ mode, then$:

$$C_{my} = 0.1 - 0.8\alpha_s = 0.818 > 0.4$$

$$k_{yy} = C_{my}\left(1 + 0.6\bar{\lambda}_y \frac{N_{Ed}}{\chi_y N_{Rk}/\gamma_{M1}}\right) = 0.835 < 0.848 = C_{my}\left(1 + 0.6\frac{N_{Ed}}{\chi_y N_{Rk}/\gamma_{M1}}\right)$$

$$k_{zy} = 0.8k_{yy} = 0.668$$

The checks:

$$\frac{N_{Ed}}{\frac{\chi_y N_{Rk}}{\gamma_{M1}}} + k_{yy}\frac{M_{y,Ed} + \Delta M_{y,Ed}}{\chi_{LT}\frac{M_{y,Rk}}{\gamma_{M1}}} = 0.714 < 1 - OK$$

$$\frac{N_{Ed}}{\frac{\chi_z N_{Rk}}{\gamma_{M1}}} + k_{zy}\frac{M_{y,Ed} + \Delta M_{y,Ed}}{\chi_{LT}\frac{M_{y,Rk}}{\gamma_{M1}}} = 0.616 < 1 - OK$$

$\Delta M_{y,Ed} = 0$ (the cross-section is doubly-symmetrical, no shift of the centroid occurs)

Therefore, the bearing capacity of the girder is sufficient.

5.4 Check of the column

The most unfavorable situation is in the case of the cross-section at the base of the column. The check will be presented for this cross-section.

The cross-section of the column is presented in Figure 5.11.

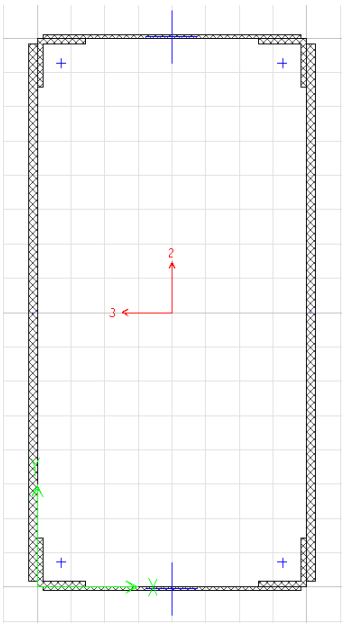

Figure 5.11 Cross-section of the column after the final rehabilitation

On the short side, the steel plates have a thickness of 3mm. On the long side, the steel plates have a thickness of 8mm. Like the girder, the cross-section of the column is class 4 and the effective properties (A_{eff}, $W_{eff,y,min}$ and $W_{eff,z,min}$) of the cross-section need to be determined. The computation of the effective properties and the checks of the column are

performed in the same way as for the girder, with the distinctions that the steel of the column angles is S235 and that the column is subjected to bi-axial bending. In the following, only the important results are presented.

5.4.1 Determination of A_{eff}

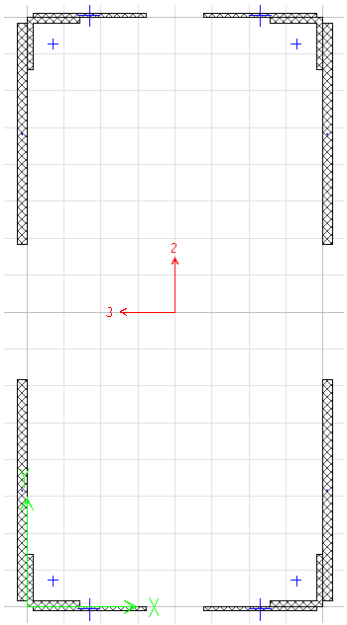

Figure 5.12 Effective cross-section of the column in case of pure compression

$A_{eff} = 7154.24mm^2$ $(considering\ only\ the\ steel\ plates)$

$N_{Rk} = 2943.96kN$

5.4.2 Determination of $W_{eff,y,min}$

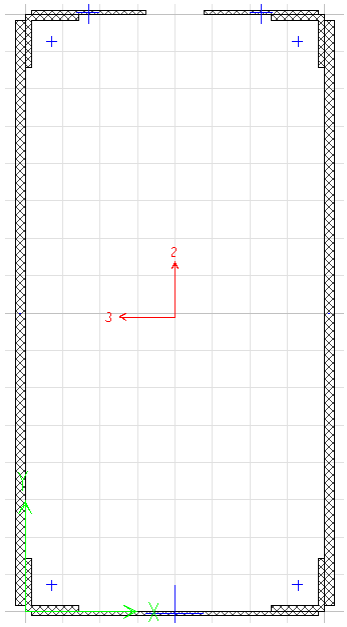

Figure 5.13 Effective cross-section of the column in case of pure bending about the major inertia axis

$W_{eff,y,min} = 931.03cm^3$ $(considering\ only\ the\ steel\ plates)$

$M_{y,Rk} = 426.39kNm$

5.4.3 Determination of $W_{eff,z,min}$

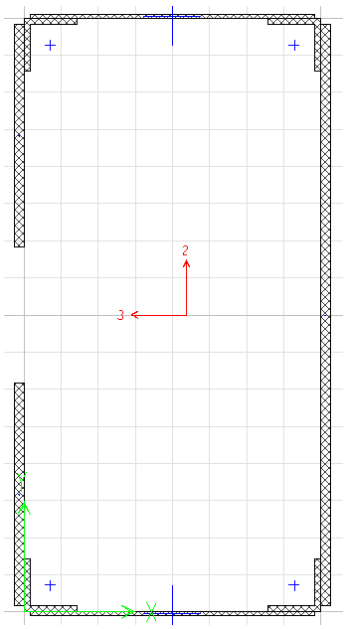

Figure 5.14 Effective cross-section of the column in case of pure bending about the minor inertia axis

$W_{eff,z,min} = 832.48cm^3$ $(considering\ only\ the\ steel\ plates)$

$M_{z,Rk} = 340.88kNm$

5.4.4 Values of the internal forces

$N_{Ed} = 75.12kN$ $(compressive)$

$V_{z,Ed} = 32.22kN$

$M_{y,Ed} = 104.39kNm$

$V_{y,Ed} = 35.6kN$

$M_{z,Ed} = 241.18kNm$

5.4.5 Resistance of the cross-section

Resistance check to axial force and biaxial bending

The check:

$$\eta_1 = \frac{N_{Ed}}{\frac{N_{Rk}}{\gamma_{M0}}} + \frac{M_{y,Ed} + N_{Ed}e_{y,N}}{\frac{M_{y,Rk}}{\gamma_{M0}}} + \frac{M_{z,Ed} + N_{Ed}e_{z,N}}{\frac{M_{z,Rk}}{\gamma_{M0}}} = 0.978 < 1 - OK$$

$e_{y,N} = e_{z,N} = 0$ (the cross-section is doubly-symmetrical, no shift of the centroid occurs)

Resistance check to shear buckling (for $V_{z,Ed}$)

The check:

$$\eta_3 = \frac{V_{Ed}}{V_{b,Rd}} = 0.021 < 1 - OK$$

$$\bar{\eta}_3 = \frac{V_{Ed}}{V_{bw,Rd}} = 0.021 < 0.5$$

Therefore, the effect of the shear force on the bending resistance does not need to be considered.

Resistance check to shear buckling (for $V_{y,Ed}$)

The check:

$$\eta_3 = \frac{V_{Ed}}{V_{b,Rd}} = 0.166 < 1 - OK$$

$$\bar{\eta}_3 = \frac{V_{Ed}}{V_{bw,Rd}} = 0.166 < 0.5$$

Therefore, the effect of the shear force on the bending resistance does not need to be considered.

5.4.6 Resistance of the member (buckling resistance)

The checks:

$$\frac{\mathrm{N_{Ed}}}{\frac{\chi_y \mathrm{N_{Rk}}}{\gamma_{M1}}} + \mathrm{k_{yy}} \frac{\mathrm{M_{y,Ed}} + \Delta \mathrm{M_{y,Ed}}}{\chi_{\mathrm{LT}} \frac{\mathrm{M_{y,Rk}}}{\gamma_{M1}}} + \mathrm{k_{yz}} \frac{\mathrm{M_{z,Ed}} + \Delta \mathrm{M_{z,Ed}}}{\frac{\mathrm{M_{z,Rk}}}{\gamma_{M1}}} = 0.558 < 1 - OK$$

$$\frac{\mathrm{N_{Ed}}}{\frac{\chi_z \mathrm{N_{Rk}}}{\gamma_{M1}}} + \mathrm{k_{zy}} \frac{\mathrm{M_{y,Ed}} + \Delta \mathrm{M_{y,Ed}}}{\chi_{\mathrm{LT}} \frac{\mathrm{M_{y,Rk}}}{\gamma_{M1}}} + \mathrm{k_{zz}} \frac{\mathrm{M_{z,Ed}} + \Delta \mathrm{M_{z,Ed}}}{\frac{\mathrm{M_{z,Rk}}}{\gamma_{M1}}} = 0.543 < 1 - OK$$

$\Delta \mathrm{M_{y,Ed}} = \Delta \mathrm{M_{z,Ed}} = 0$ (the cross-section is doubly-symmetrical, no shift of the centroid occurs)

Therefore, the bearing capacity of the column is sufficient.

5.5 Check of the welds of the steel plates

The steel plates are welded to the angles as presented in Figure 5.15.

Figure 5.15 Welds between the steel plates and the angles

The check is presented for the girder. The check is performed similarly for the column, with the distinction that it is subjected to bi-axial bending.

The welds are checked with respect to the sliding force, which depends on the static moment of the area that slides longitudinally. Two checks need to be performed (1 check for the welds of the flange and 1 check for the welds of the webs). However, it is sufficient to perform only the second check as the sliding force is greater in this case due to the fact that the static moment of the area that slides longitudinally is greater in this case; for the first case, the static moment is given only by the flange, while for the second case, the static moment is given by the flange and the two angles.

$S_y(z) = 385.07cm^3 \ - static\ moment\ of\ the\ area\ that\ slides\ longitudinally$

$I_y = 24564.8cm^4$

$V_{z,Ed} = 140.19kN$

$F_{w,Ed} = \frac{S_y(z)}{I_y} \cdot V_{z,Ed} = 219.76N/mm \ - design\ value\ of\ the\ sliding\ force$

$f_{vw,d} = \frac{f_u}{\sqrt{3} \cdot \beta_w \cdot \gamma_{M2}} = 207.85N/mm^2$

$a = a_{min} = 3mm - \ thickness\ of\ the\ weld$

$F_{w,Rd} = 4 \cdot f_{vw,d} \cdot a = 2494.2N/mm\ (accounting\ for\ 4\ welds\ on\ one\ side)$

The check:

$F_{w,Ed} = 219.76N/mm \ < F_{w,Rd} = 2494.2N/mm \ - OK$

5.6 Check of the vertical deflection

$f_{max} = 25.5mm < 42mm = \frac{L}{250} = f_{adm} - OK$

5.7 Check of the seismic lateral drift for the SLS

$\nu = 0.5$

$d_{re} = 28.3mm$

$d_r^{SLS} = \nu q d_{re} = 14.2mm$

$h = 6.775m$

$d_{r,a}^{SLS} = 0.005h = 33.9mm$

$d_r^{SLS} = 14.2mm < 33.9mm = d_{r,a}^{SLS} - OK$

5.8 Check of the seismic lateral drift for the ULS

$d_{re} = 28.3mm$

$d_r^{ULS} = cq\, d_{re} = 28.3mm$

$h = 6.775m$

$d_{r,a}^{ULS} = 0.025h = 169.4mm$

$d_r^{ULS} = 28.3mm < 169.4mm = d_{r,a}^{ULS} - OK$

5.9 Evaluation of the girder-to-column node

In order to validate the rehabilitation solution, a GMNIA was performed on the girder-to-column node. The numerical model is presented in Figure 5.16.

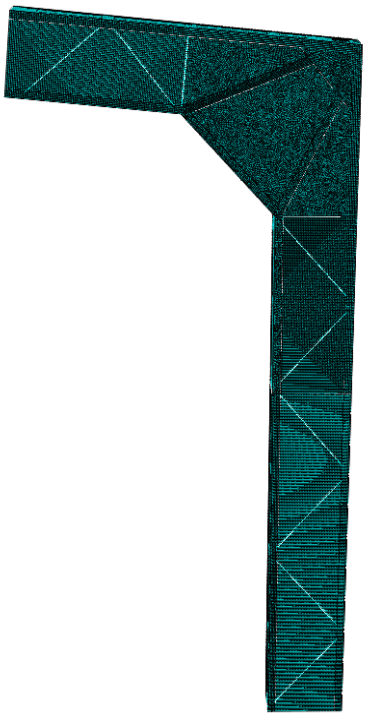

Figure 5.16 Numerical model of the girder-to-column node after the final rehabilitation

13 different models were considered (1 model without imperfections and 12 models with different cases of imperfections) in order to determine the most unfavorable situation. The imperfections are applied by first performing an eigen buckling analysis. Following the buckling analysis, it resulted that the eigen buckling modes are given by the local buckling of

the steel plates (each eigen buckling mode represents the local buckling of the steel plates of either the girder or the column). The shape of the imperfections is applied according to the considered buckling mode with the amplitude e_0 computed according to Eurocode 3-1-5 (See Figure 5.17).

Type of imperfection	Component	Shape	Magnitude
global	member with length ℓ	bow	see EN 1993-1-1, Table 5.1
global	longitudinal stiffener with length a	bow	min (a/400, b/400)
local	panel or subpanel with short span a or b	buckling shape	min (a/200, b/200)
local	stiffener or flange subject to twist	bow twist	1 / 50

Figure 5.17 Design value of the imperfection [11]

The imperfection study is presented in Figure 5.18. The number in the name of each model represents the eigen buckling mode according to which the imperfections are applied (in the case of "Imp 1", the imperfections are applied according to the first buckling mode).

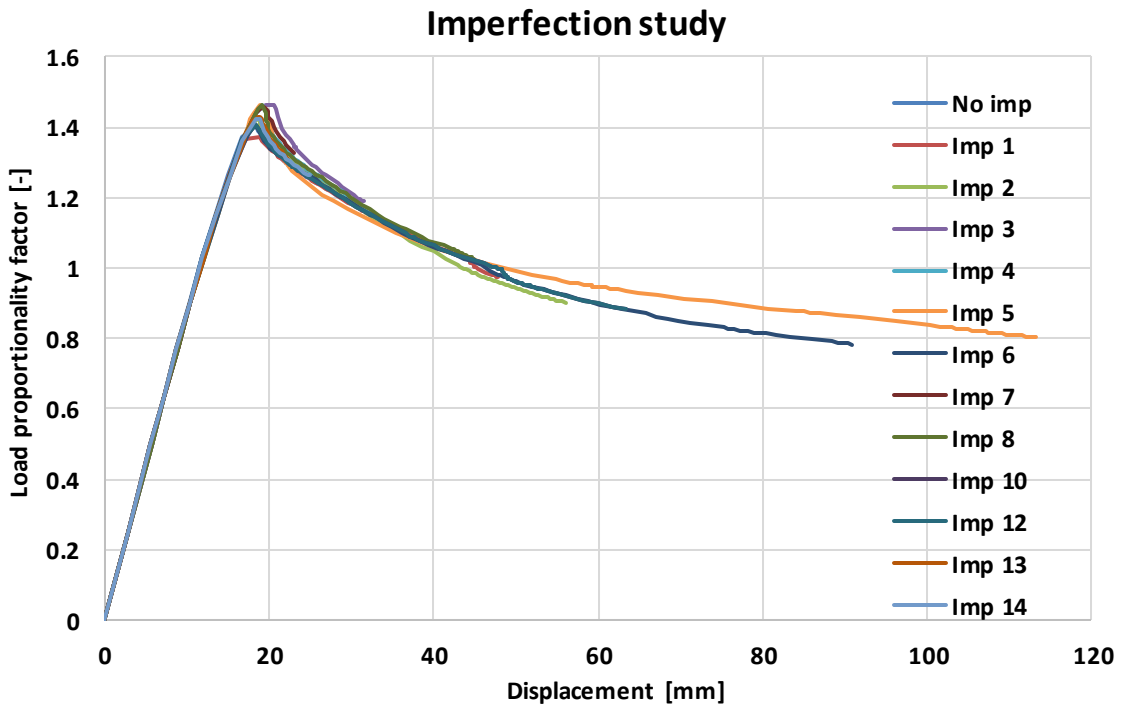

Figure 5.18 Imperfection study for the node after the final rehabilitation

The most unfavorable situation is in the case when the imperfections are applied according to the first buckling mode. The results are further presented for this case.

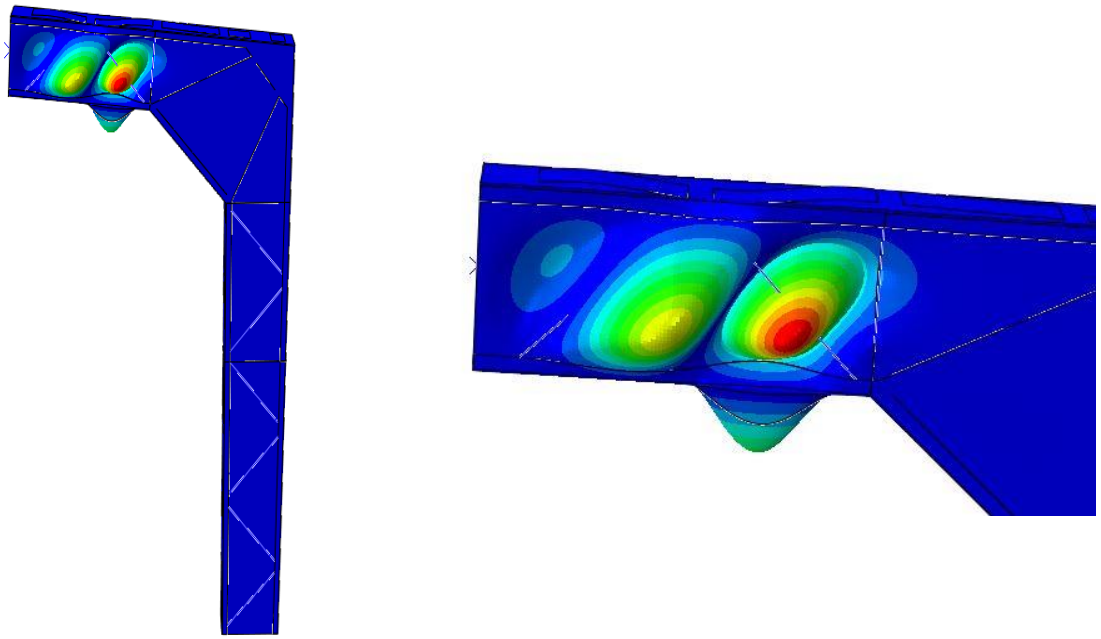

(a) General view of the node *(b) Close-up of the region where the buckling occurs*

Figure 5.19 The first buckling mode of the node after the final rehabilitation

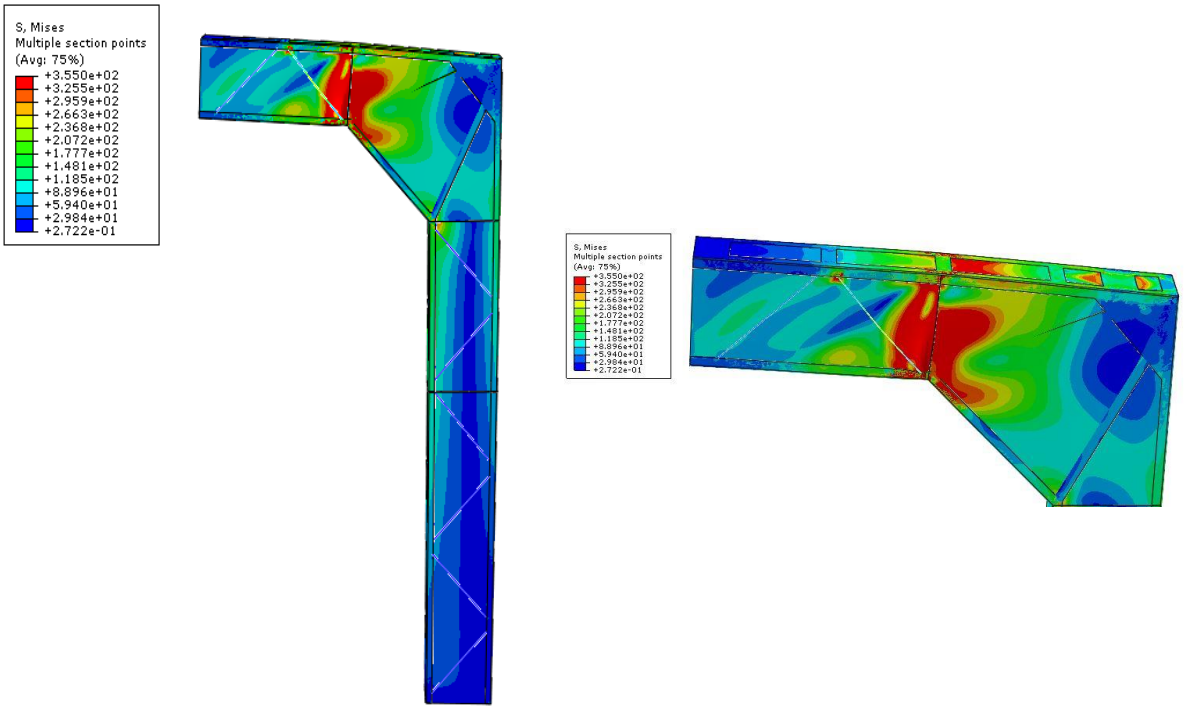

(a) General view of the node *(b) Close-up of the region where the failure occurs*

Figure 5.20 The distribution of von Mises stresses and the deformed shape of the node after the final rehabilitation

The failure of the node occurs due to the failure in shear buckling of the girder and node web steel plates. This failure mechanism can be explained by considering that the web steel plates are slender, making them susceptible to the phenomenon of shear buckling. Moreover, the failure occurs close to the end of the node, where the value of the shear force is maximum. Even in the analytical check of the girder, the check to shear buckling proved to be significant (See Paragraph 5.3.4).

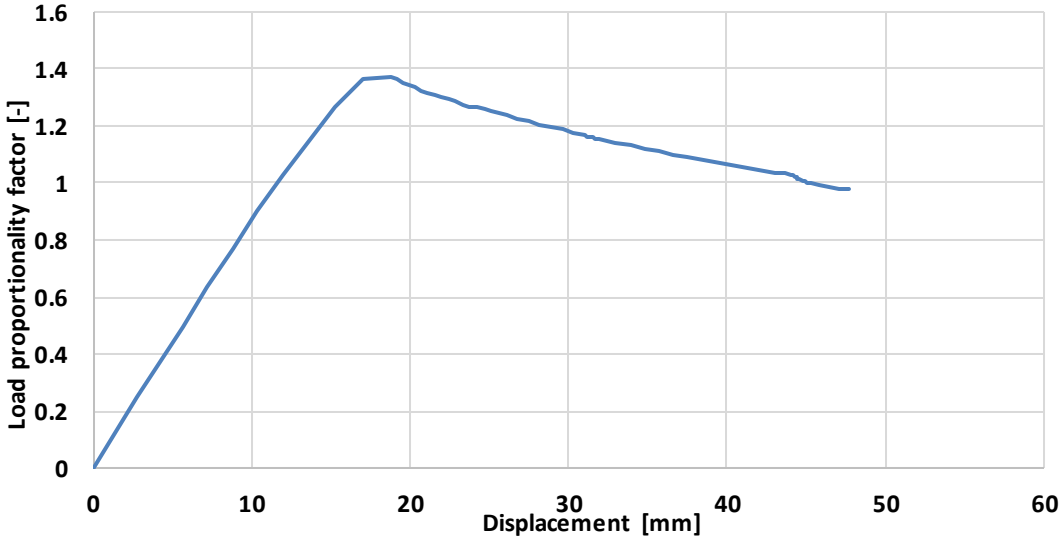

Figure 5.21 Load proportionality factor of the node after the final rehabilitation

As the value of the Load Proportionality Factor is 1.37, the bearing capacity of the node is sufficient.

The comparison between the rehabilitated node and the initial node is presented in Figure 5.22. The bearing capacity of the node is increased almost 6 times following the structural upgrade.

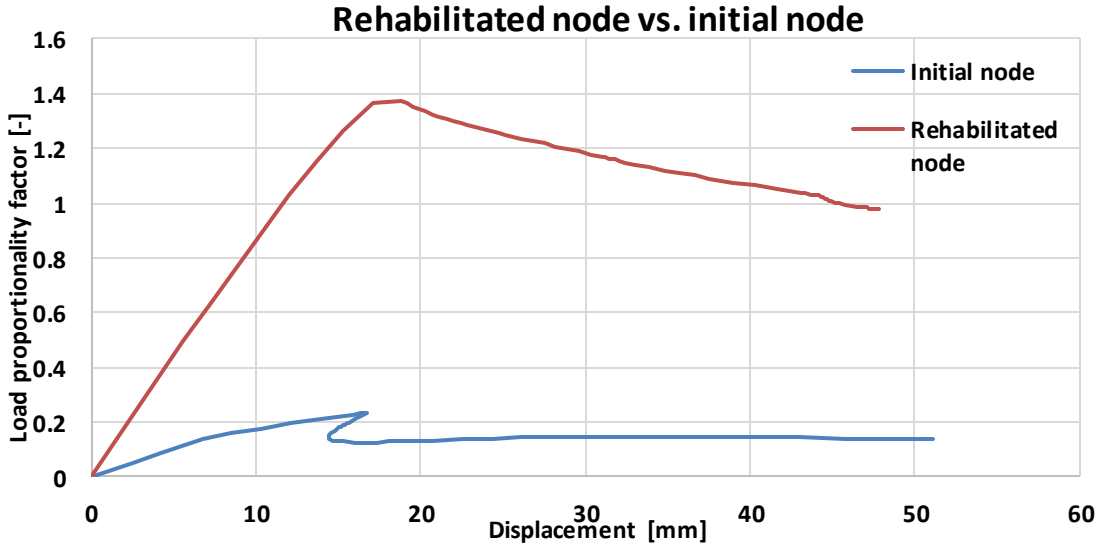

Figure 5.22 Comparison between the initial node and the rehabilitated node

6 CONCLUSIONS

The assessment of the initial structure revealed that the bearing capacity of the structure is greatly exceeded. This is due to the fact that the current design codes operate with higher climate (snow and wind) and seismic loads than the codes at the time of design. Therefore, in order to extend the service life of the structure and reuse it, a structural upgrade is necessary.

The structure was partially rehabilitated after it was damaged during the September 2017 storm. However, the aim of this partial rehabilitation was only to restore the initial bearing capacity of the damaged frames and to ensure the structural safety in the case of the normal use of the structure (no snow load acting on the structure), the need for a structural upgrade still existing.

As the proposed rehabilitation solution was validated and due to the fact that the rehabilitation solution can be applied without interrupting the laboratory activities within the hall, the adaptive reuse objective is achieved. The rehabilitation solution implies a steel consumption of 1.35t/transversal frame (8.1t in total, respectively 25.7kg/m^2). However, as previously mentioned, the aim of the thesis was not to provide the solution that would lead to the smallest steel consumption (which would be the demolition of the structure and the erection of a new one, but for which the laboratory work cannot be performed), but to provide a rehabilitation solution (with a reasonable steel consumption) that would accomplish the goal of adaptive reuse.

7 REFERENCES

[1] Fujita, M., Iwata, M., "The reuse management model of building steel structures", Proceedings of EUROINFRA Conference, Helsinki, Finland, 2009.

[2] Gorgolewski, M., Straka, V., Edmonds, J., Sergio, C., "Facilitating greater reuse and recycling of structural steel in the construction and demolition process", Department of Architectural Science, Faculty of Engineering and Applied Science, Final Report, Ryerson University, Canada, 2006.

[3] Research Fund for Coal and Steel, RFCS-02-2016, Proposal No. 747847, "PROGRESS".

[4] Research Fund for Coal and Steel, RFCS-02-2016, Proposal No. 747847, "PROGRESS", Deliverable D1.1, Factsheets on review of existing deconstruction cases, November 2017.

[5] Research Fund for Coal and Steel, RFCS-02-2016, Proposal No. 747847, "PROGRESS", Reuse of Steel Case Study no. 5, "Design of the in-situ rehabilitation of the Steel Structures Laboratory of PUT".

[6] SCIENTIFIC BULLETIN of the "POLITEHNICA" University of Timisoara, Romania, Transactions on CIVIL ENGINEERING and ARCHITECTURE, Editura POLITEHNICA, 2009.

[7] Mateescu, D., Gadeanu, L., Mercea, G., Muhlbacher, R., Cosmulescu, P., "Constructii Metalice", Editura Didactica si Pedagogica, Bucuresti.

[8] EN 1991-1-3 (2005), Eurocode 1: Actions on structures – Part 1-3: General actions – Snow loads.

[9] EN 1991-1-4 (2005), Eurocode 1: Actions on structures – Part 1-4: General actions – Wind actions.

[10] EN 1993-1-1 (2005), Eurocode 3: Design of steel structures – Part 1-1: General rules and rules for buildings, CEN, European Committee for Standardization.

[11] EN 1993-1-5 (2005), Eurocode 3: Design of steel structures – Part 1-5: Plated structural elements, CEN, European Committee for Standardization.